

CHAPTER IV

RESULTS AND DISCUSSION

4.1 Preliminary Study

In the preliminary study, the chitosan/carrageenan beads were prepared in various coagulant solutions. The coagulant solution consists of NaOH for the precipitation of chitosan, and KCl for carrageenan ionotropic gelation. The time and temperature of the bead immersion in the coagulant solutions were also varied. The suitable conditions that give the optimal of drug loading efficiency were selected for the next experiment.

The percentage of loading efficiency (%LE) in each chitosan/carrageenan bead formulation is given in Table 4.1. The chitosan/carrageenan beads were prepared in different concentrations of NaOH solution (Formulation P1, P2 and P3 in Table 4.1). The increase in NaOH concentration resulted in the increase in %LE of the beads. In spite of this, the concentration of NaOH solution should not exceed 7.5 % (w/v), as it becomes difficult to remove any excess NaOH and also difficult to neutralize. Therefore, in this study, the optimum concentration of NaOH is 5.0% (w/v). When we compared the temperature of the coagulant solution (Formulation P2 and P4), the coagulant solution maintained at 10°C gave a better %LE (94.90%) than the one maintained at room temperature (88.12%).

In order to determine the effects of KCl concentration in the coagulant solution on the production of stable well formed chitosan/carrageenan beads, the concentrations of KCl were varied from 0 to 0.5M in 5% NaOH, at 10°C for 5 hours (Formulation of P2, P5, P6 and P7). The results showed that the %LE was improved after the addition of KCl to the coagulant solution. Moreover, the highest %LE (96.20%) was obtained after 0.3M KCl was added (Formulation P6),

corresponding to the preparation of the pure carrageenan beads reported by Cassidy et al.^[41] and López et al.^[42].

The %LE also depends on the coagulant time. The beads immersed in the coagulant solution (5% NaOH, 0.3M KCl, 10°C) for 3 hours eroded during filtering, washing and freeze drying process. The beads were well formed when the immersion time was 5 hours. As the bead immersion time increased from 5 to 24 hours, the amount of drug loss also increased by approximately 5%. Thus, the suitable coagulant condition used in the next experiment was 5% NaOH/0.3M KCl maintained at 10°C with the bead immersion time of 5 hours.

Table 4.1 Drug loading efficiency (LE) of the chitosan/carrageenan bead in the preliminary study of coagulant solutions

Formulation	NaOH conc. (%w/v)	KCl conc. (M)	Temp.	Time	%LE ^a ± S.D. ^b
P1	2.5	-	10°C	5 h	88.39±0.17
P2	5.0	-	10°C	5 h	94.90±0.28
P3	7.5	-	10°C	5 h	96.53±0.50
P4	5.0	-	RT	5 h	88.12±0.26
P5	5.0	0.1	10°C	5 h	95.63±0.12
P6	5.0	0.3	10°C	5 h	96.20±0.90
P7	5.0	0.5	10°C	5 h	96.20±0.34
P8	5.0	0.3	10°C	3 h	- ^c
P9	5.0	0.3	10°C	overnight	91.69±0.17

^a %LE = The percentage of drug loading efficiency was studied using indirect method.

^b S.D. = Standard deviation

^c The %LE was not shown because the beads were fragile and the shape was not well formed and broken into pieces after drying.

4.2 Characterization and Physical Properties

4.2.1 Morphology of the beads

The observation of size, shape and surface topography of the dried beads were conducted by scanning electron microscopy (SEM). The results were separated into groups of the beads with varying ratios of chitosan/carrageenan, DFNa content, type and amount of cross-linking agent. The microscopic images were taken in three magnifications for each formulation as illustrated in Figures 4.1-4.9.

The sizes of the beads for each formulation as varied from 2 to 3 millimeters shown in Table 4.2. The size distribution was affected by the composition of the formulation.

Figures 4.1, 4.2 and 4.3 show the scanning electron photomicrographs of the beads produced by various chitosan/carrageenan ratios (1/0, 3/1, 2/1 and 1/1) in different magnifications. These beads were not completely spherical. They had a rough and folded surface due to the shrinking during the freeze drying process. Especially, the surface of the beads from formulation C, which were prepared from chitosan/carrageenan ratio of 2/1, was rougher and more porous than the others (Figure 4.2). The cross-section view of these beads are shown in Figure 4.3. The cavities inside the beads increased as the ratios of carrageenan in the beads increased.

Table 4.2 The sizes of the beads obtained with various compositions as determined by scanning electron microscopy

Formulation	CS/CR ratio	DFNa content (%W/V)	Crosslinking agent		Bead size \pm S.D. ^a (mm)
			(%W/V)		
			GA	GD	
A	1/0	1	-	-	2.14 \pm 0.19
B	3/1	1	-	-	2.43 \pm 0.12
C	2/1	1	-	-	2.44 \pm 0.14
D	1/1	1	-	-	2.51 \pm 0.26
E	1/2	1	-	-	nd
F	1/3	1	-	-	nd
G	0/1	1	-	-	nd
H	2/1	-	-	-	2.31 \pm 0.16
I	2/1	2	-	-	2.05 \pm 0.25
J	2/1	3	-	-	2.16 \pm 0.19
K	2/1	4	-	-	2.34 \pm 0.12
L	2/1	5	-	-	2.66 \pm 0.18
M ^b	2/1	5	1.00	-	nd
N	2/1	5	-	1.00	nd
O	2/1	5	0.25	-	2.55 \pm 0.16
P	2/1	5	0.50	-	2.55 \pm 0.19
Q	2/1	5	0.75	-	2.60 \pm 0.36
R ^c	2/1	5	1.00	-	2.90 \pm 0.23
S	2/1	5	-	5.00	3.09 \pm 0.12

^a S.D. = Standard deviation

^b The beads were crosslinked by the first method.

^c The beads were crosslinked by the second method.

nd (not determined) ; because the beads were not successfully prepared.

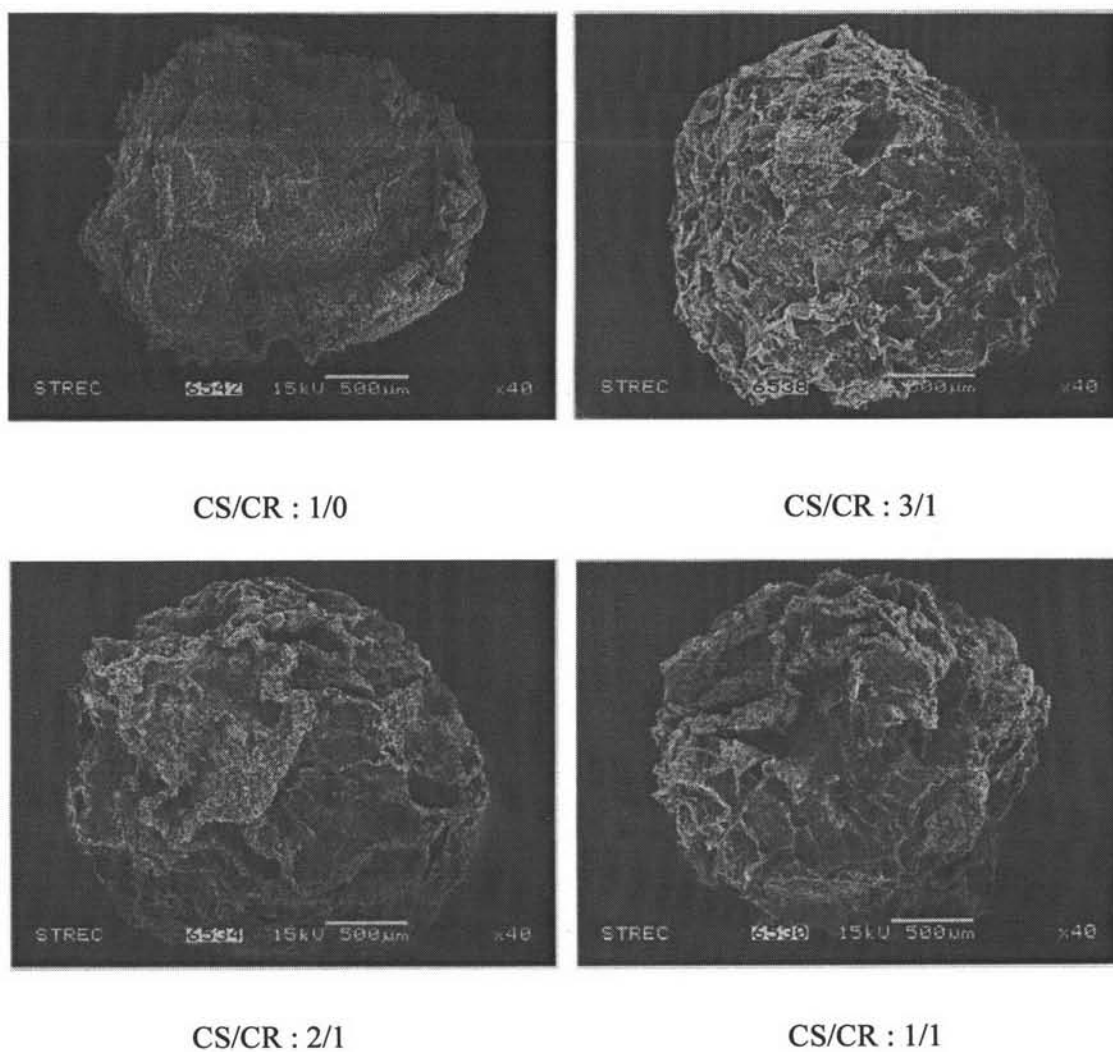


Figure 4.1 Scanning electron photomicrographs of the beads with various weight ratios of chitosan/carrageenan (1/0, 3/1, 2/1 and 1/1) with DFNa content at 1% (w/v); (x40).

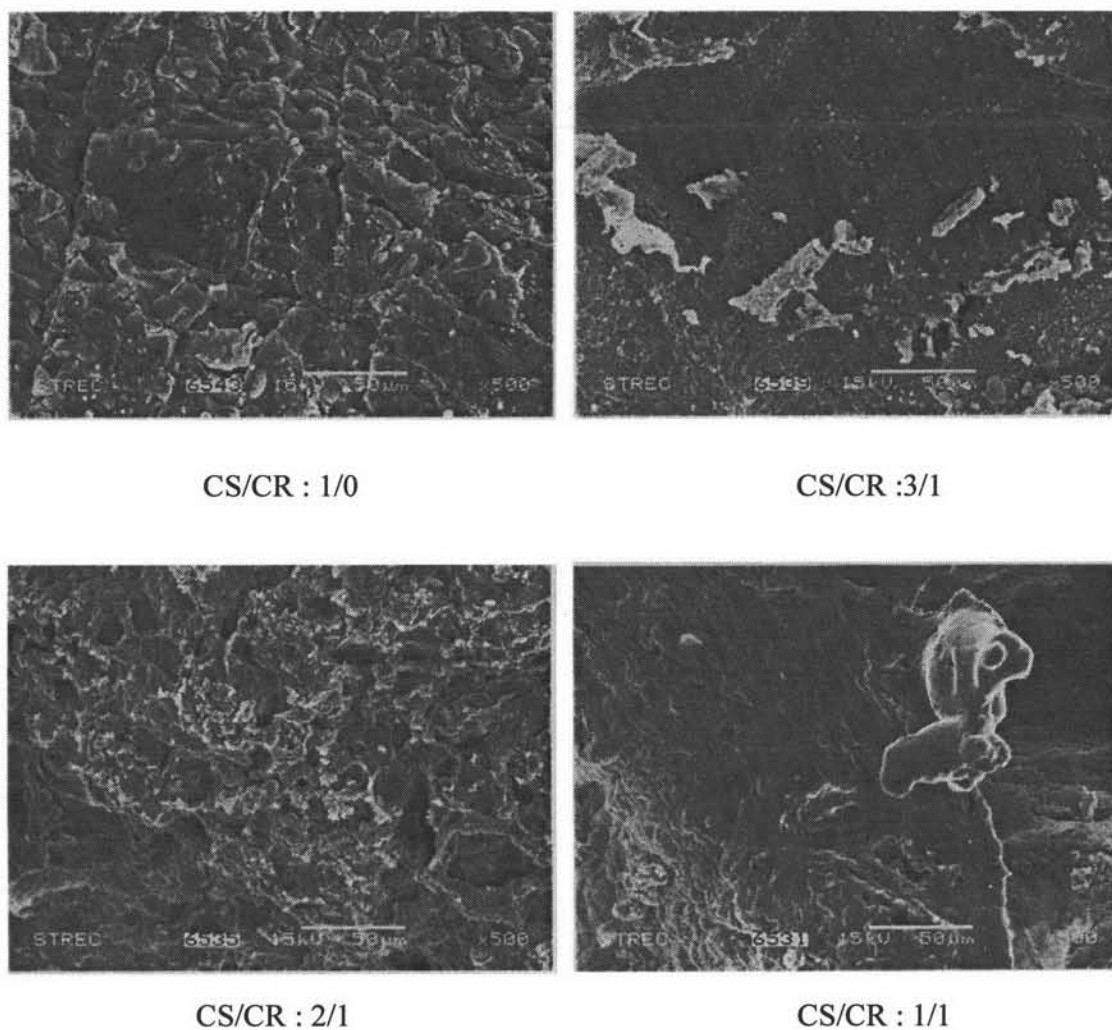


Figure 4.2 Scanning electron photomicrographs at surface of the beads with various weight ratios of chitosan/carrageenan (1/0, 3/1, 2/1 and 1/1) with DFNa content at 1% (w/v); (x500).

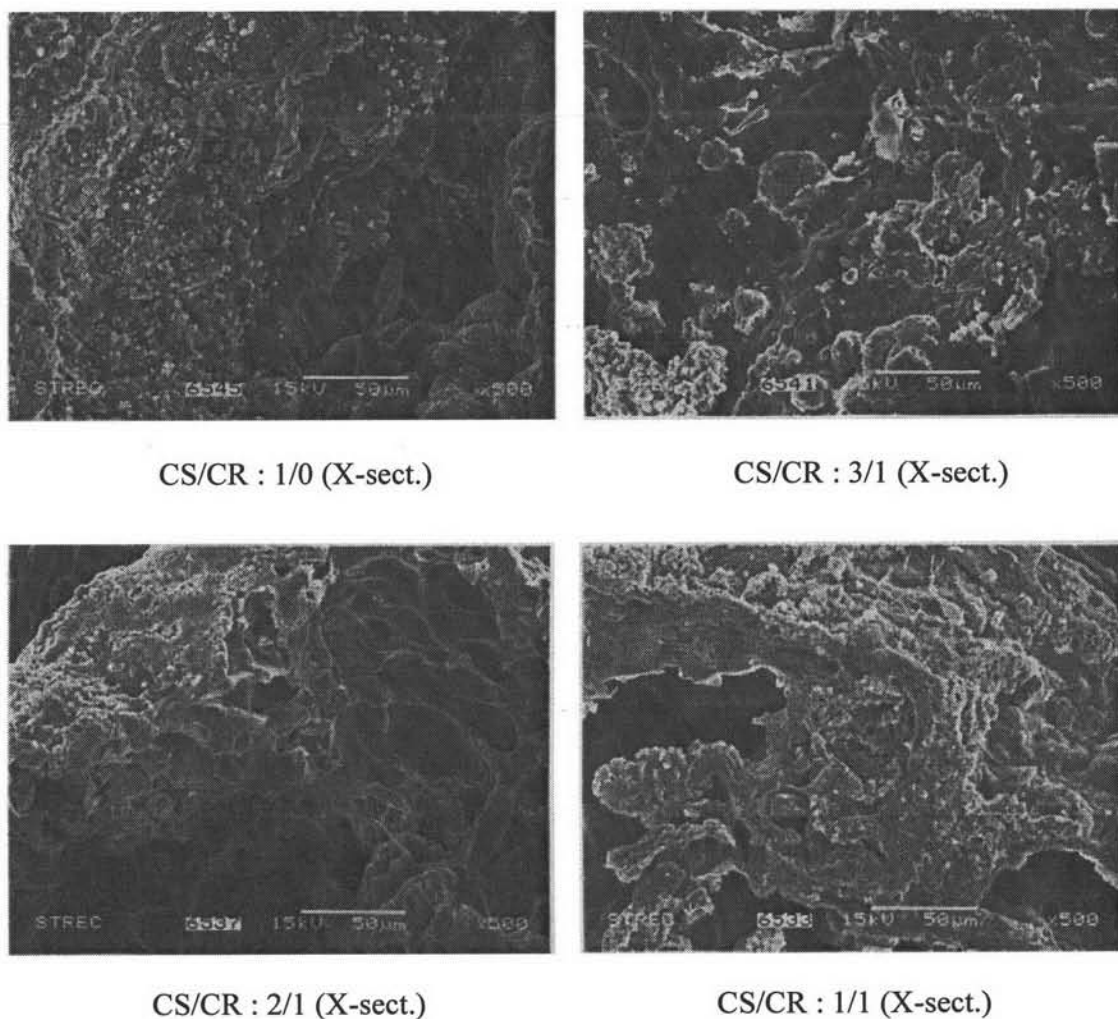


Figure 4.3 Scanning electron photomicrographs of cross-section of the beads with various weight ratios of chitosan/carrageenan (1/0, 3/1, 2/1 and 1/1) with DFNa content at 1% (w/v); (x500).

The photomicrographs of the chitosan/carrageenan (CS/CR : 2/1) beads with varying in DFNa content (1-5% (w/v)) in different magnifications are shown in Figures 4.4, 4.5 and 4.6. The photomicrographs of the bead without DFNa content shows that the bead was partly shrunk. When the DFNa content in the beads increased, the size of beads increased and their surface was covered with irregular crystals of DFNa. The cross-section view of the beads with various DFNa content are shown in Figure 4.6.

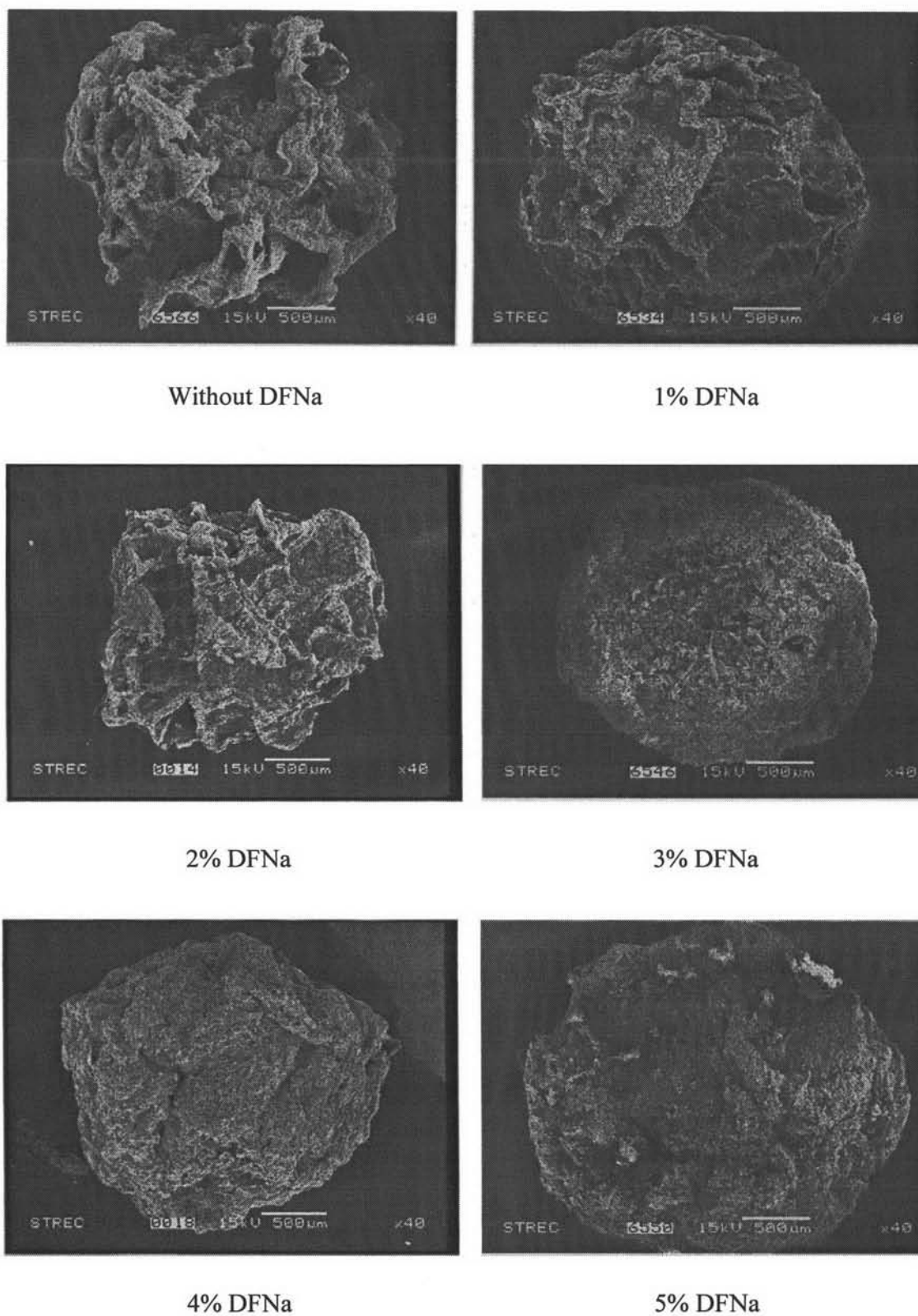


Figure 4.4 Scanning electron photomicrographs of the chitosan/carrageenan (CS/CR : 2/1) bead without DFNa and the beads with various DFNa content of 1%, 2%, 3%, 4% and 5% (w/v); (x 40).

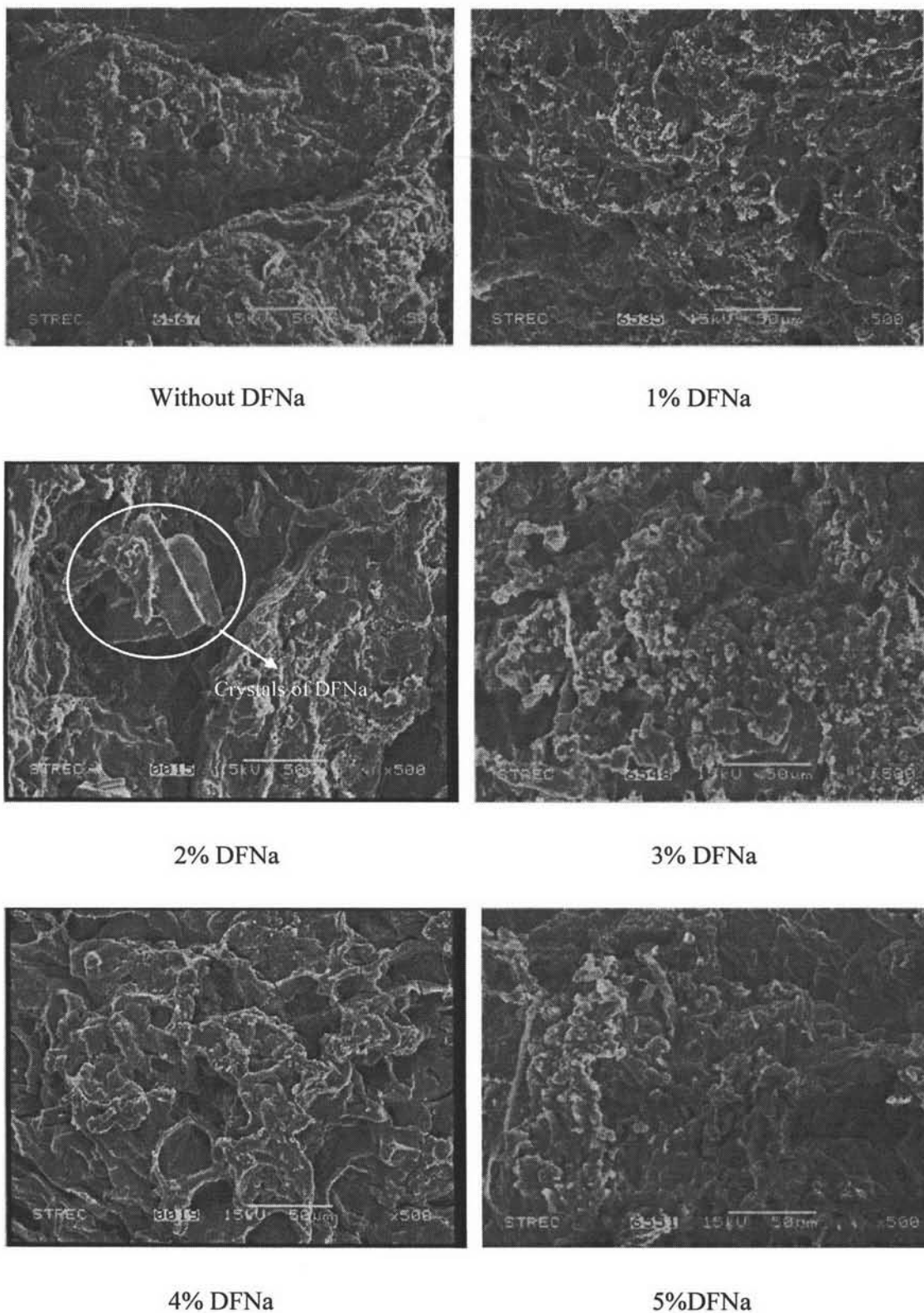
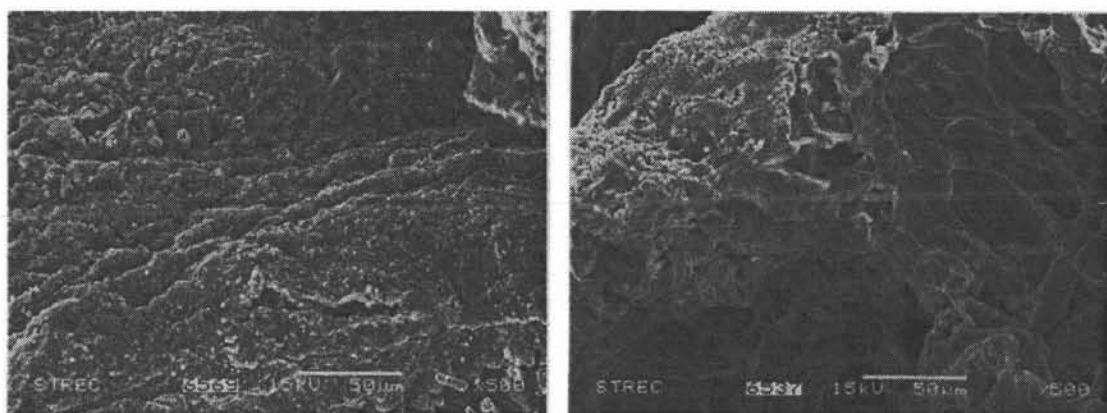
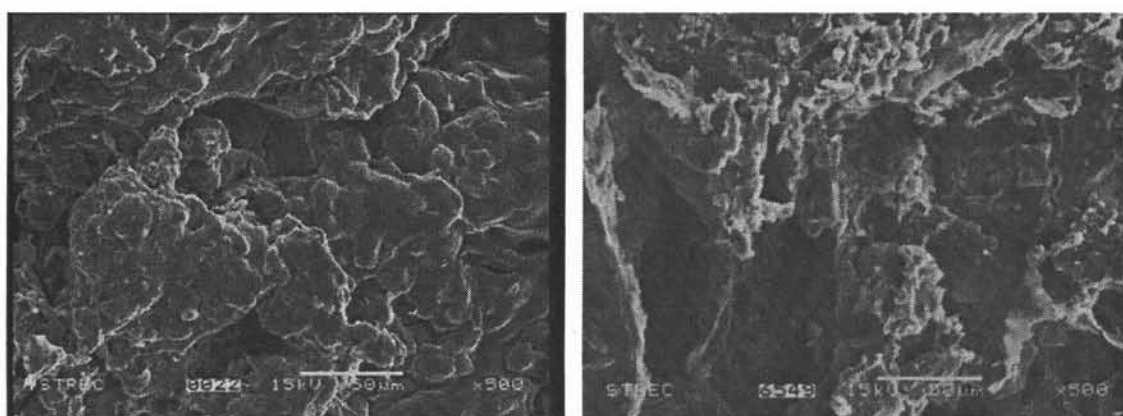


Figure 4.5 Scanning electron photomicrographs at surface of the chitosan/carrageenan (CS/CR : 2/1) bead without DFNa and the beads with various DFNa content of 1%, 2%, 3%, 4% and 5% (w/v); (x 500).



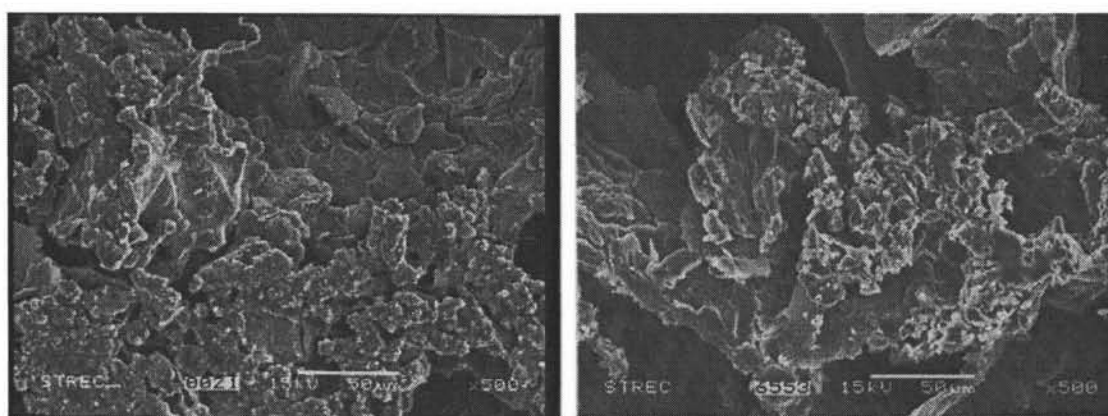
Without DFNa (X-sect.)

1% DFNa (X-sect.)



2% DFNa (X-sect.)

3% DFNa (X-sect.)



4% DFNa (X-sect.)

5% DFNa (X-sect.)

Figure 4.6 Scanning electron photomicrographs of cross-section of the chitosan/carrageenan (CS/CR : 2/1) bead without DFNa and the beads with various DFNa content of 1%, 2%, 3%, 4% and 5% (w/v); (x 500).

Figures 4.7, 4.8 and 4.9 represent the photomicrographs of the cross-linked bead obtained from various concentrations of glutaric acid at 0.25-1.00% (w/v) and glutaraldehyde at 5.00% (w/v). These beads were prepared by the same ratio of chitosan/carrageenan (CS/CR : 2/1) with 5% (w/v) DFNa. The beads crosslinked with glutaric acid at different concentrations show irregular shapes and rough moon-liked surfaces. The cross-section views of these beads are shown in Figure 4.9.

The beads that were crosslinked with 5.00% (w/v) glutaraldehyde exhibit spherical shape and larger than the others, presumably because the bead had shrunk minimally during the freeze-drying process. The surface of the bead was smooth and was less porous than the others, resulting in the difficulty for dissolution medium to penetrate into the bead. Therefore, this may reduce the efficiency of the drug release as well.

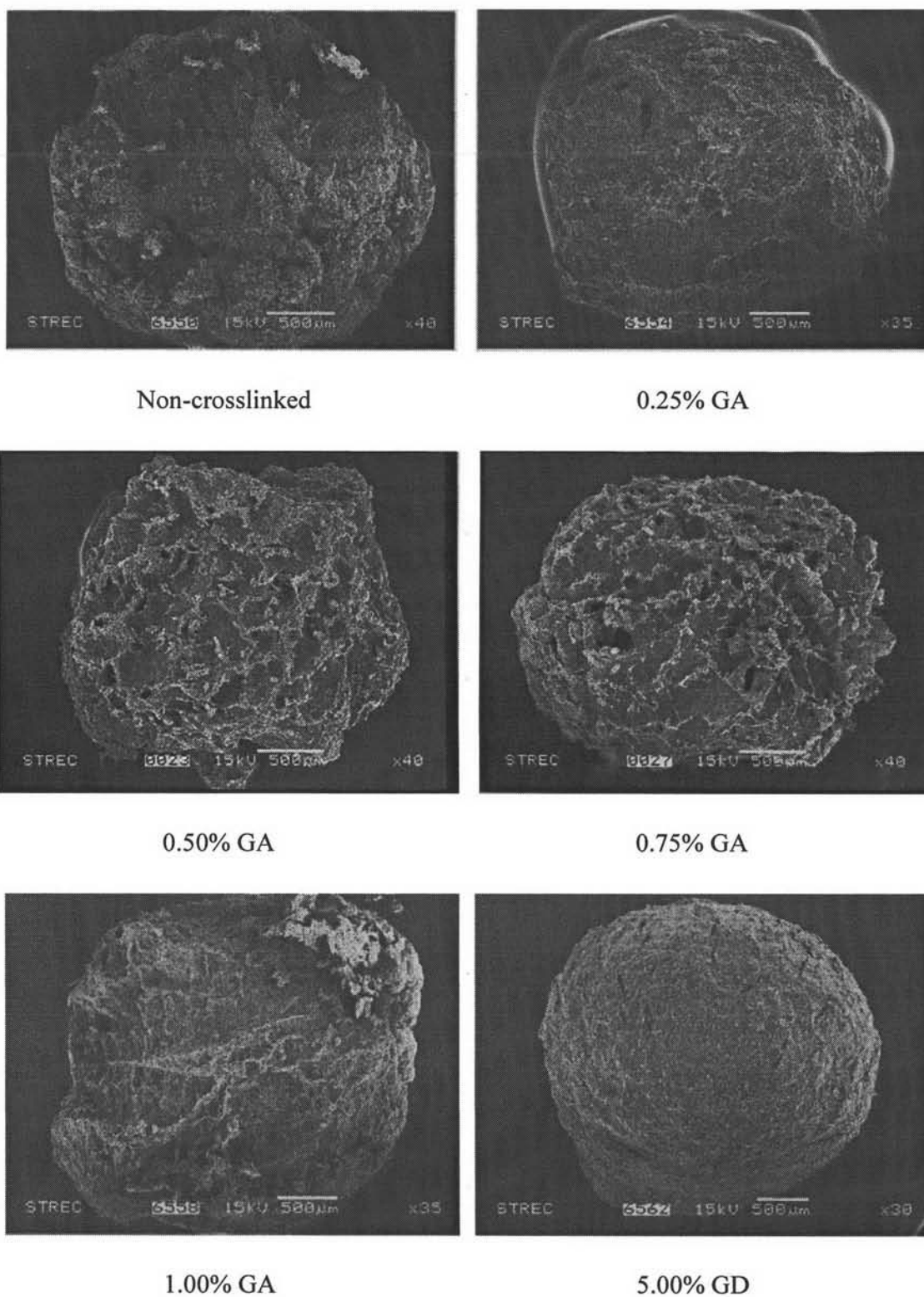


Figure 4.7 Scanning electron photomicrographs of the non-crosslinked beads (CS/CR : 2/1, DFNa content at 5% (w/v)) and the beads crosslinked with different concentration of crosslinking agent; 0.25-1.00% (w/v) glutaric acid (GA) and 5.00% (w/v) glutaraldehyde (GD) at different magnifications.

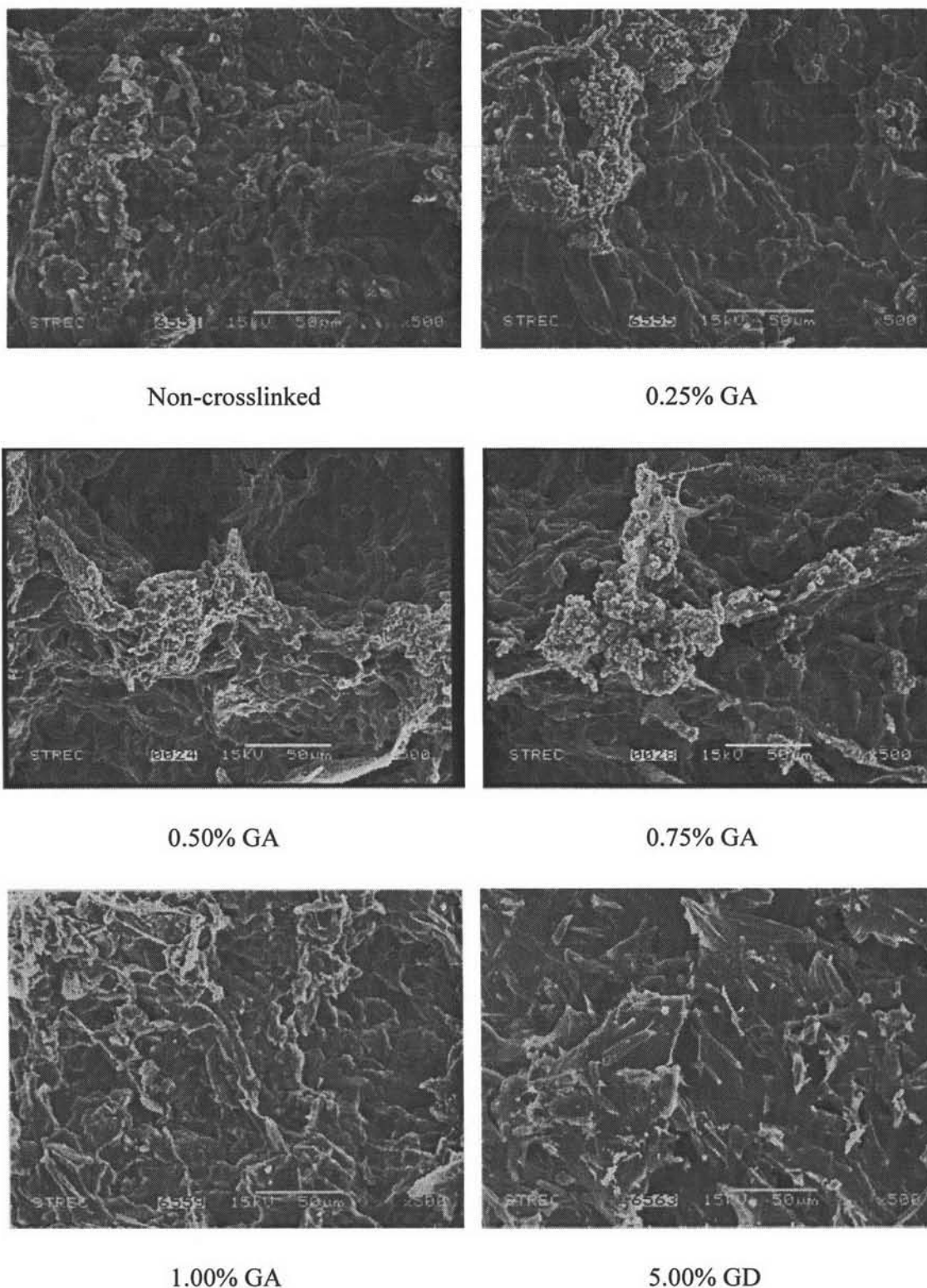
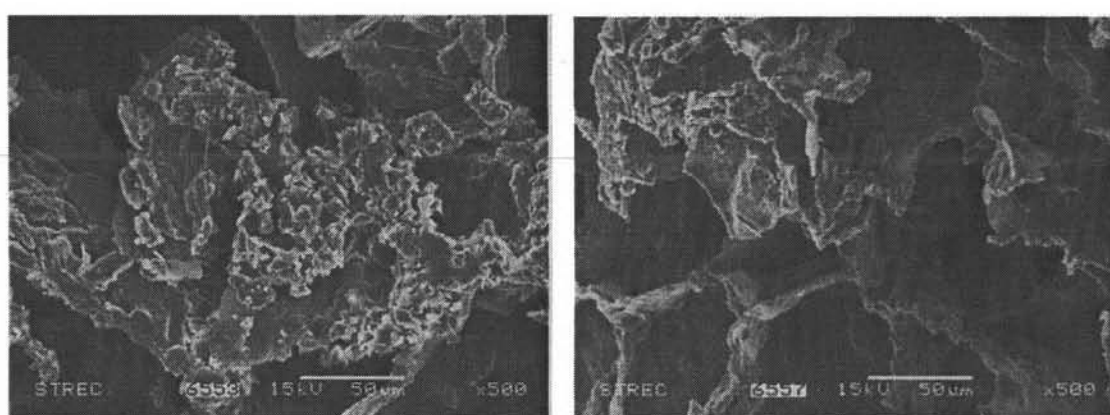
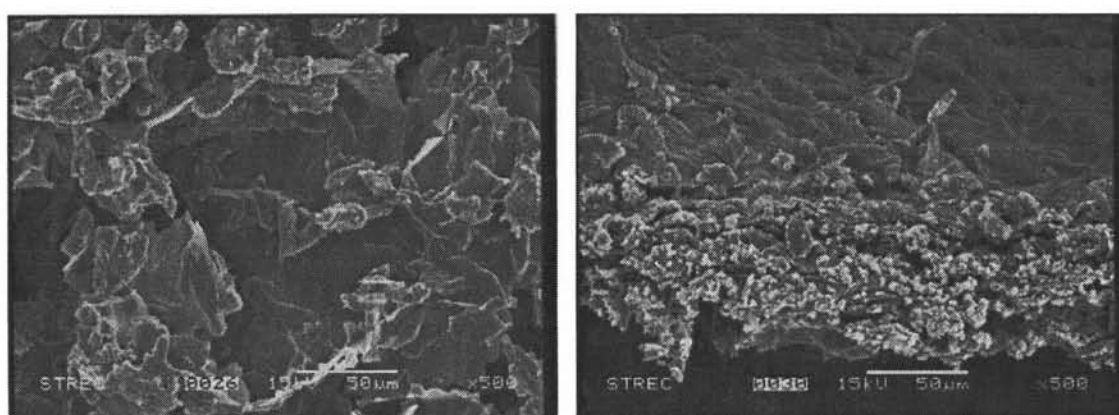


Figure 4.8 Scanning electron photomicrographs at surface of the non-crosslinked beads (CS/CR : 2/1, DFNa content at 5% (w/v)) and the beads crosslinked with different concentration of crosslinking agent; 0.25-1.00% (w/v) glutaric acid (GA) and 5.00% (w/v) glutaraldehyde (GD);(x 500).



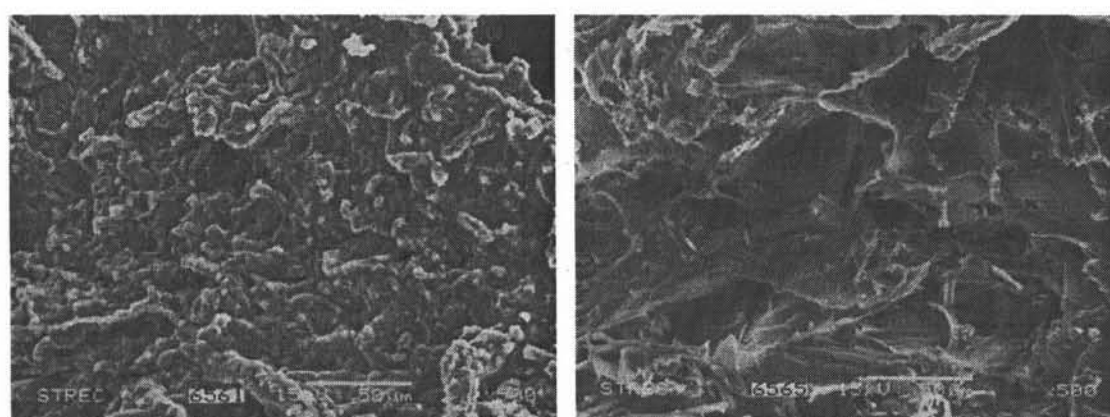
Non-crosslinked (X-sect.)

0.25% GA (X-sect.)



0.50% GA (X-sect.)

0.75% GA (X-sect.)



1.00% GA (X-sect.)

5.00% GD (X-sect.)

Figure 4.9 Scanning electron photomicrographs of cross-section of the non-crosslinked beads (CS/CR : 2/1, DFNa content at 5% (w/v)) and the beads crosslinked with different concentration of crosslinking agent; 0.25-1.00% (w/v) glutaric acid (GA) and 5.00% (w/v) glutaraldehyde (GD);(x 500).

4.2.2 Fourier transform infrared spectroscopy (FT-IR)

The IR spectrum of the tested samples are shown in Figures 4.10-4.13. Figure 4.10 (a) shows the IR spectrum of chitosan. The peaks were observed at 1587, 1653, 2871 and 3416 cm^{-1} . The peak at 1587 cm^{-1} resulted from N-H bending. The IR absorption peak at 1653 and 2871 cm^{-1} correspond to C=O of amide groups and $-\text{CH}_3$ stretching respectively. These two peaks represent a fraction of chitin that were not hydrolyzed. The broad band at 3416 cm^{-1} resulted from N-H stretching combined with $-\text{OH}$ stretching.

Figure 4.10 (b) shows the IR spectrum of carrageenan. The peaks were observed at 707, 765, 855, 1018 and 3396 cm^{-1} . The characteristic peaks for galactose sulfate are shown in the crowded fingerprint region at 707, 765, 855 and 929 cm^{-1} [43]. The peak at 1018 cm^{-1} resulted from sulfate ester group and the broad band at 3396.76 cm^{-1} resulted from $-\text{OH}$ stretching.

Figure 4.10 (c) shows the IR spectrum of chitosan/carrageenan (CS/CR) bead. The spectrum showed a new absorption at 1450 cm^{-1} which displaces peak of NH_2 at 1587 cm^{-1} together with a decreased in intensity of $-\text{SO}_4^{2-}$ group absorption band at 1018 cm^{-1} . The appearance of the new absorption band at 1450 cm^{-1} can be assigned to $-\text{NH}_3^+$ group and the strong reduction in intensity of the absorption band of $-\text{SO}_4^{2-}$ group is the evidence for the formation of strong polyelectrolyte complex (PEC).

Figure 4.11 (b) shows the IR spectrum of DFNa. The principle peaks were observed at 746, 765, 1279, 1302, 1501 and 1575 cm^{-1} . The peaks at 746 and 765 cm^{-1} resulted from C-H out of plane bending. The IR absorption bands at 1279 and 1302 cm^{-1} resulted from C-N stretching and the peak at 1501 and 1575 cm^{-1} resulted from C=C stretching and C=O stretching of carboxylate group, respectively.

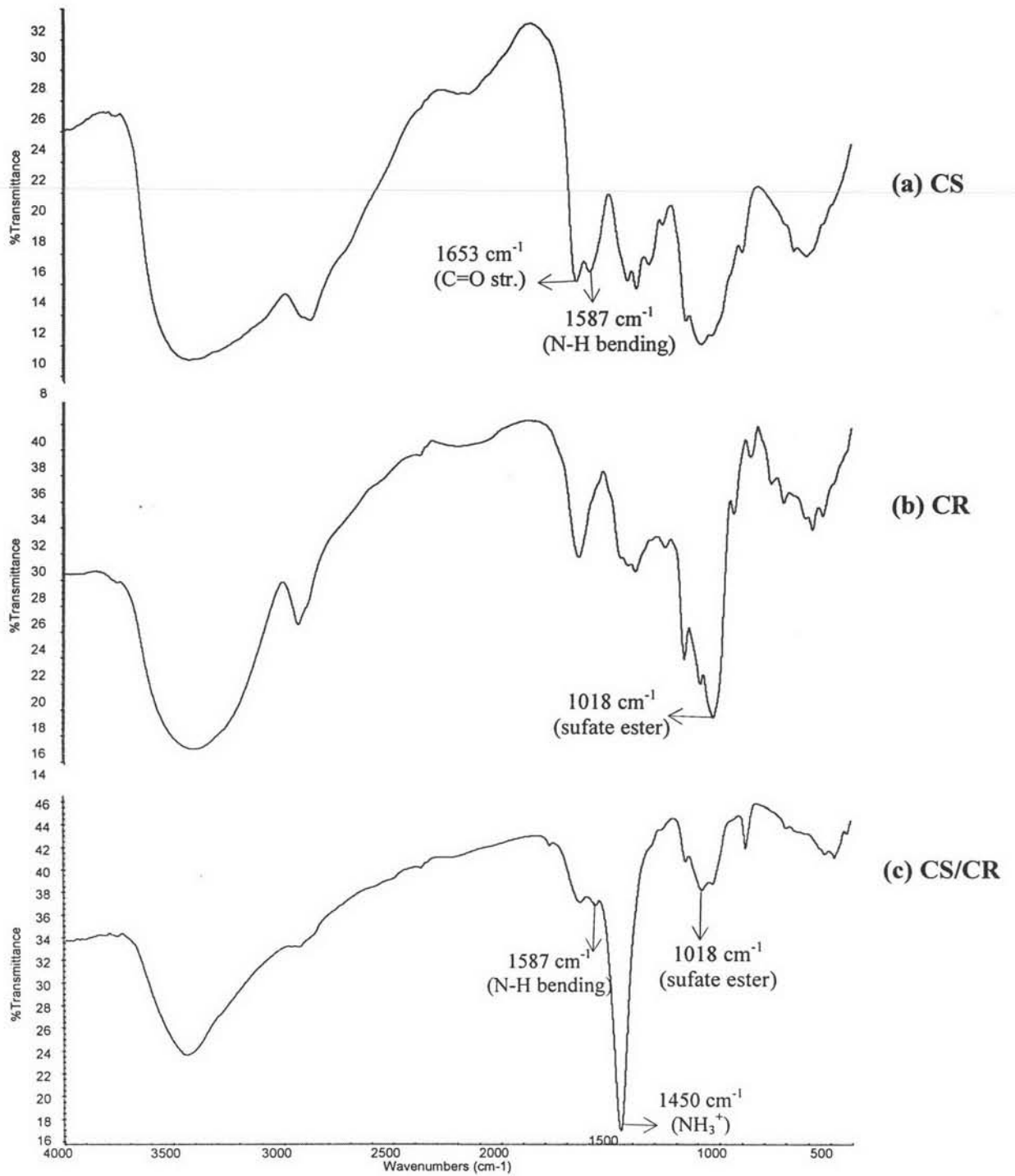


Figure 4.10 FT-IR spectra of (a) chitosan (CS), (b) carrageenan (CR), and (c) CS/CR bead.

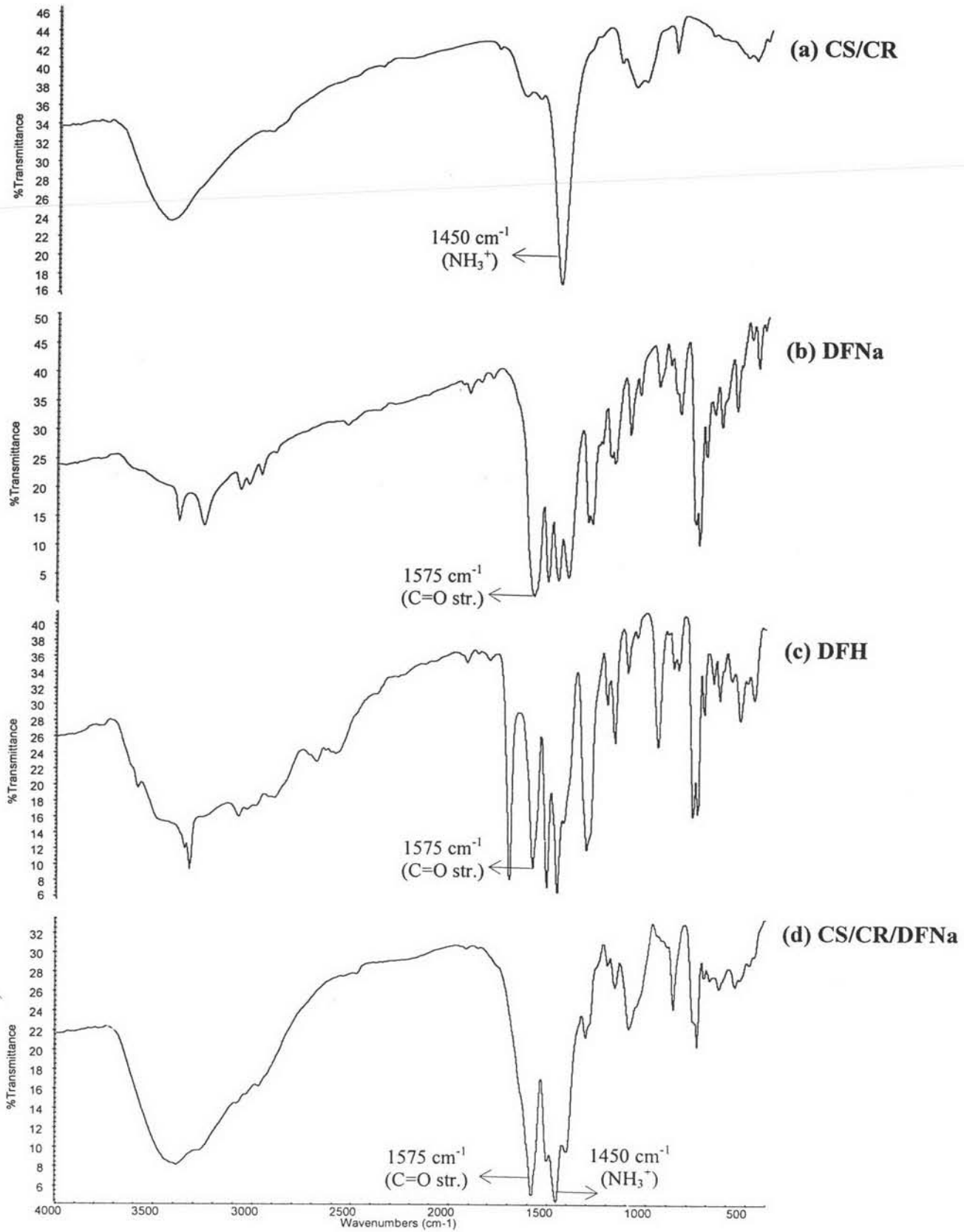


Figure 4.11 FT-IR spectra of (a) CS/CR bead, (b) DFNa, (c) DFH and (d) CS/CR/DFNa bead.

Figure 4.11 (c) displays the IR spectrum of DFH. DFNa can be converted into DFH (diclofenac acid) in acidic solution. The peak for C=O of carboxylic acid was found at 1575 cm^{-1} and the peak for free -OH group was found at 3315 cm^{-1} .

The IR spectrum of DFNa-loaded chitosan/carrageenan beads is shown in Figure 4.11 (d). The spectrum of the bead showed a combination of peak from both polymer matrix and drug, while the principle peaks of polymer matrix and drug were also present. The positions of peaks were not shifted from original material. It could be concluded that interactions between polymer matrix and drug were unlikely to occur and type of matrix former had no effect on the IR spectra.

Figure 4.12 (b) displays the IR spectrum of DFNa-loaded chitosan/carrageenan beads crosslinked with glutaric acid. The IR absorption peak of the bead crosslinked with glutaric acid showed an increase in the intensity of C=O group absorption at 1575 cm^{-1} and showed a decrease in the intensity of -NH_3^+ group absorption band at 1450 cm^{-1} which indicate the ionic crosslinking between -NH_3^+ groups of chitosan and -COO^- groups of glutaric acid.

The IR spectrum of DFNa-loaded chitosan/carrageenan beads crosslinked with glutaraldehyde is shown in Figure 4.12 (c). The intensity of the absorption peak for -NH_3^+ of chitosan at 1450 cm^{-1} decreased and appearance of a new peak at 1696 cm^{-1} resulting due to the formation of imine linkage (-C=N-) between the amino groups of chitosan and the C=O groups of the glutaraldehyde.

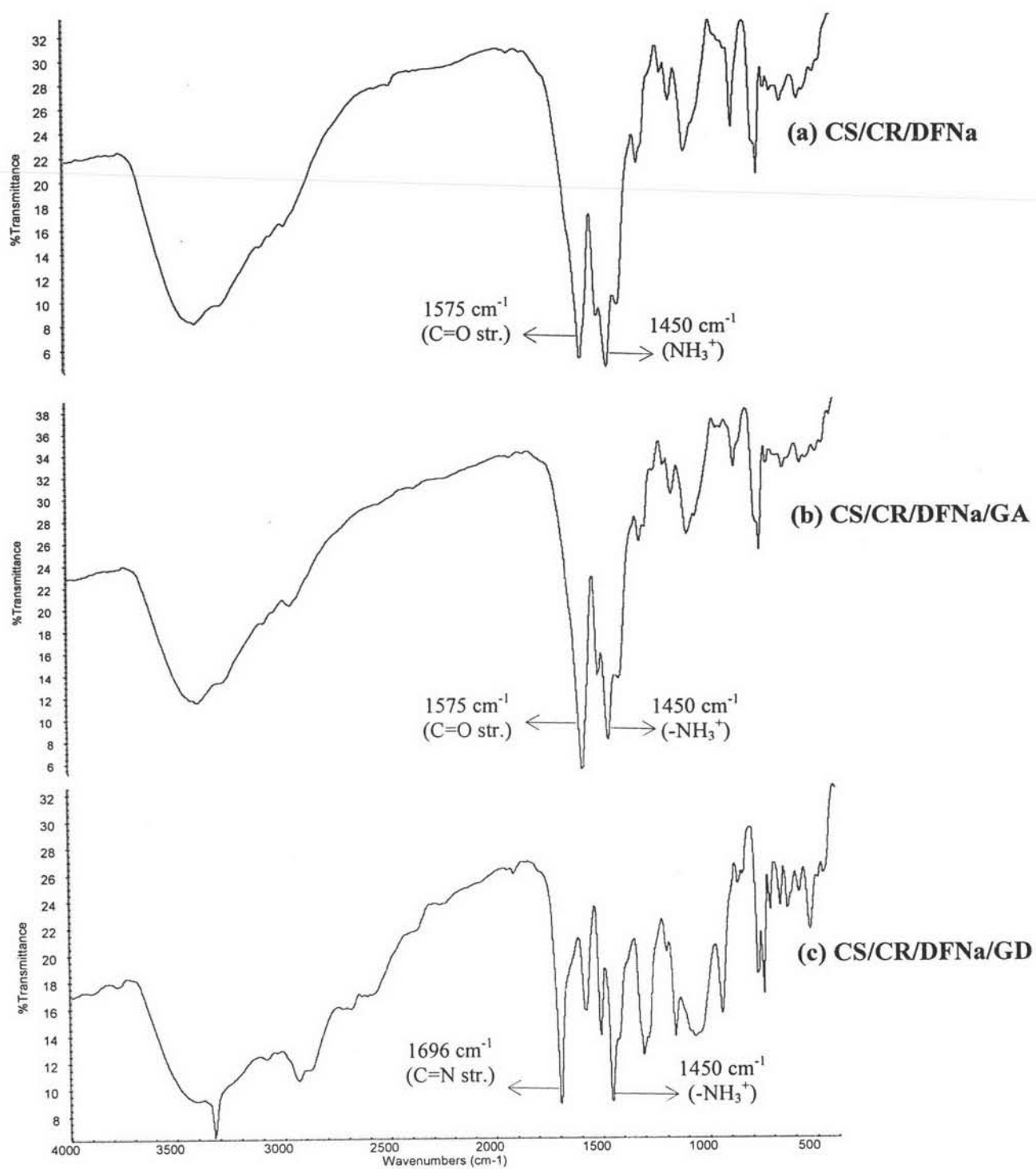


Figure 4.12 FT-IR spectra of (a) CS/CR/DFNa, (b) CS/CR/DFNa/GA and (c) CS/CR/DFNa/GD bead.

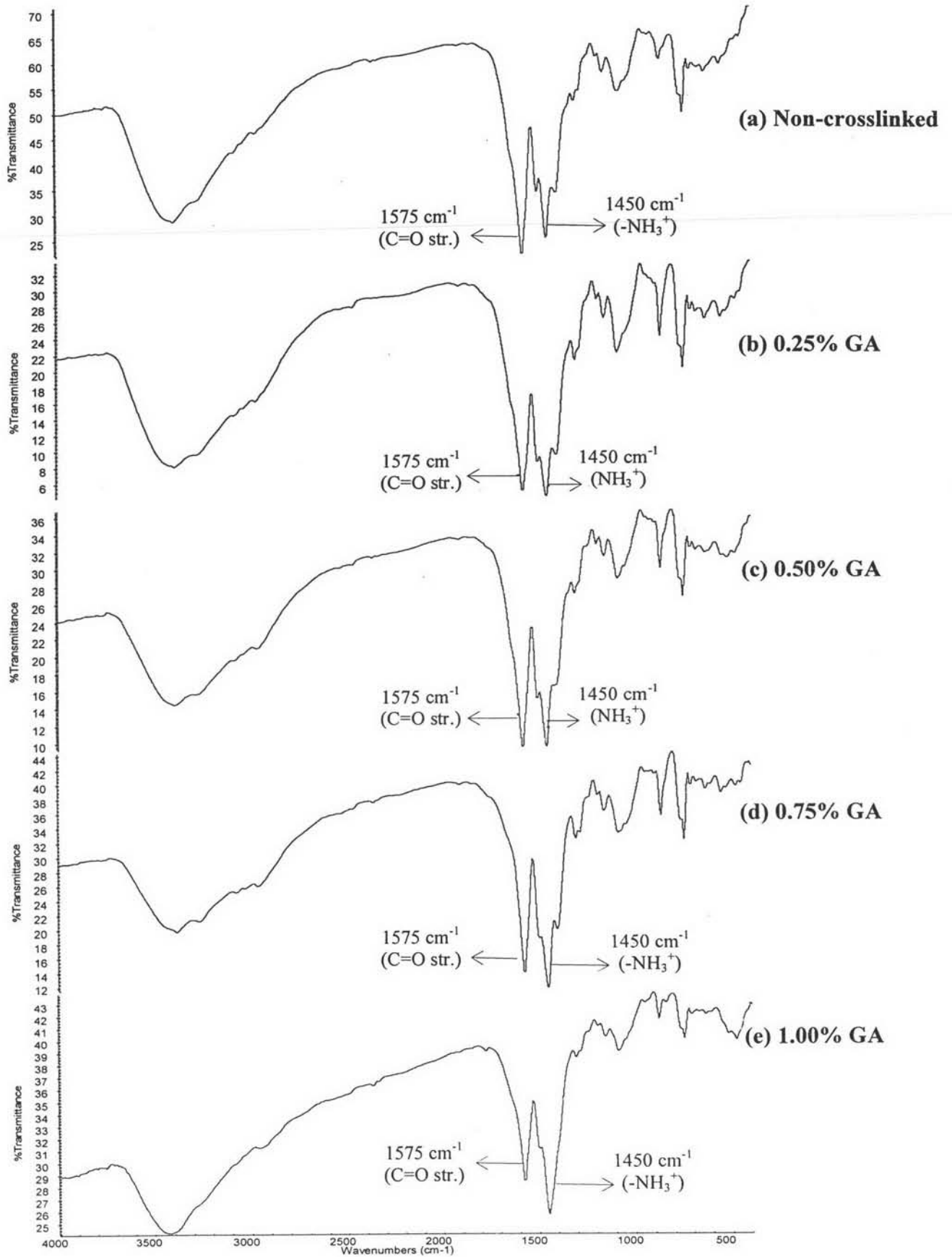


Figure 4.13 FT-IR spectra of (a) the non-crosslinked chitosan/carrageenan beads and the beads crosslinked with glutaric acid at (b) 0.25%, (c) 0.50%, (d) 0.75% and (e) 1.00% (w/v).

Figure 4.13 (a-e) shows the IR spectra of the beads that were crosslinked with glutaric acid at different concentrations. These spectra are of similar pattern but different in the intensity of C=O and -NH_3^+ peaks. In the bead crosslinked with 0.25% (w/v) glutaric acid, the intensity of -NH_3^+ peak was lower than that of the non-crosslinked bead because -NH_3^+ groups of chitosan had ionic interaction with -COO^- groups of glutaric acid. When the concentrations of glutaric acid were increased from 0.25% (w/v) to 0.50-1.00% (w/v), the negatively charged groups of glutaric acid were increasingly repelled. Therefore, the ionic interaction between -NH_3^+ groups of chitosan and -COO^- groups of glutaric acid were decreased, resulting in the increase of the intensity of -NH_3^+ peak.

4.2.3 Thermal analysis

4.2.3.1 Differential scanning calorimetry (DSC)

Chitosan, carrageenan, DFNa and the beads obtained from various compositions were analysed with the differential scanning calorimeter. The DSC thermograms of pure chitosan, pure carrageenan and the chitosan/carrageenan bead are shown in Figure 4.14 (a-c). The pure chitosan bead revealed an endothermic peak at 86.3°C and an exothermic peak at 262.4°C. These two peaks represent the evaporation of water and the degradation of chitosan, respectively. The pure carrageenan bead showed a broad endothermic peak at 72.5°C and a sharp endothermic peak at 265.0°C before a fusion with degradation at 269.0°C. The chitosan/carrageenan bead shows a higher endothermic peak, at 92.5°C, and lower exothermic peak at 196.0°C, than those of the pure substances. The lower exothermic peak of chitosn/carrageenan indicated the presence of the polyelectrolyte complex (PEC) between chitosan and carrageenan. Similar thermal stability behavior has been reported by de Paula et al. [44].

Figure 4.15(b) represents the DSC thermogram of pure DFNa showing two endothermic peaks. The first smaller endothermic, at 63.0°C, was due to water loss. The second sharp endothermic peak at 288.0°C and an exothermic peak at 296.0°C can be attributed to the fusion of the solvated crystals and oxidation reaction between DFNa and oxygen in air environment, respectively [45].

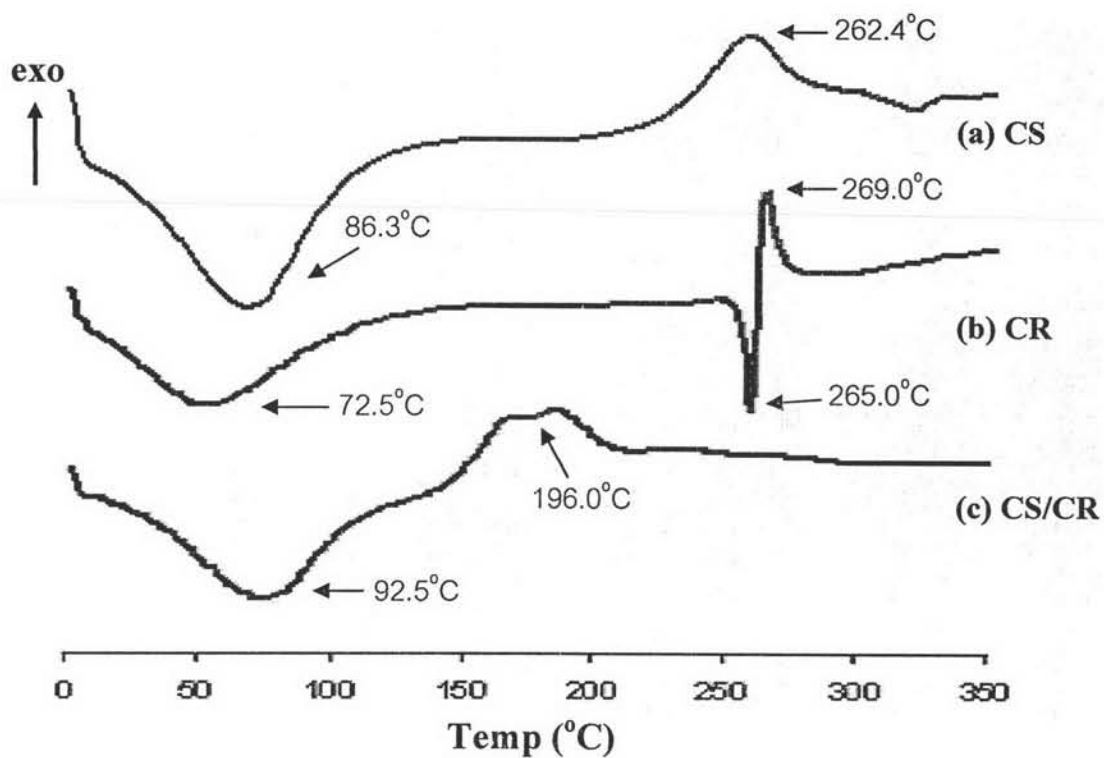


Figure 4.14 DSC thermograms of (a) chitosan (CS), (b) carrageenan (CS) and (c) CS/CR bead.

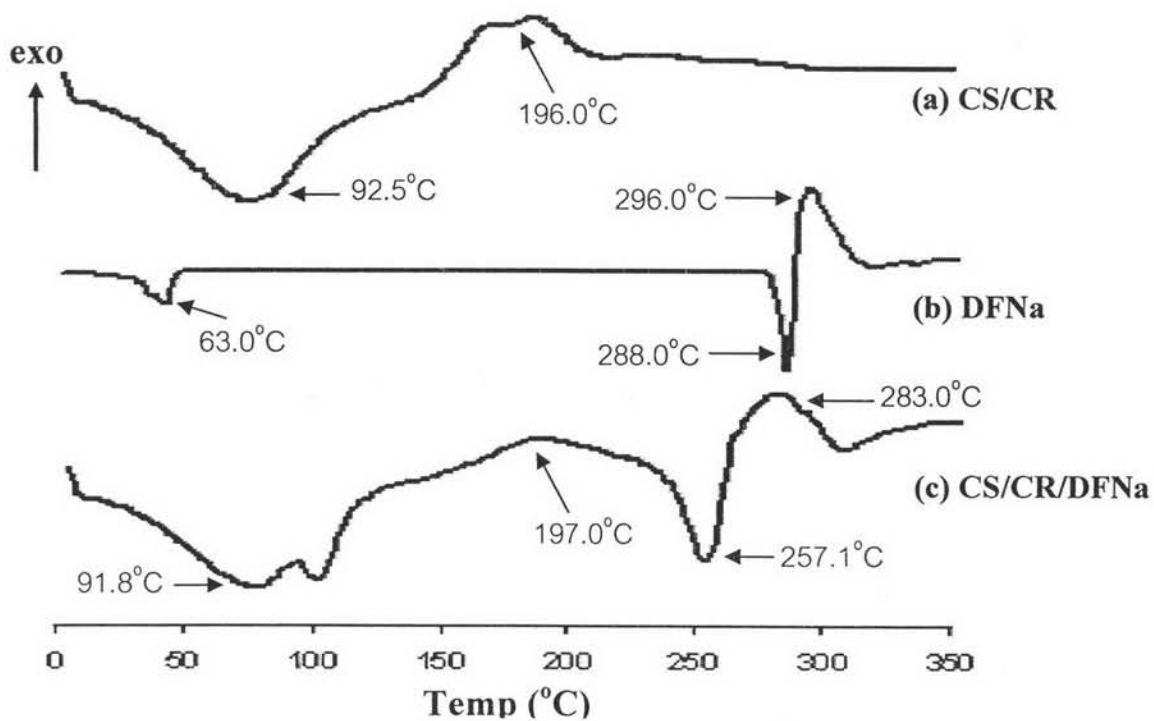


Figure 4.15 DSC thermograms of (a) CS/CR, (b) sodium diclofenac (DFNa) and (c) CS/CR/DFNa bead.

The DSC thermograms of the chitosan/carrageenan bead and the DFNa-loaded chitosan/carrageenan bead are compared in Figure 4.15 (a) and (c). The thermogram of the DFNa-loaded chitosan/carrageenan bead displays a combination of polymer and drug thermograms. The characteristic peak of the chitosan/carrageenan bead and DFNa were also still present but slightly shifted from their original position. This indicated that the interaction between the drug and the polymer bead was unlikely to occur.

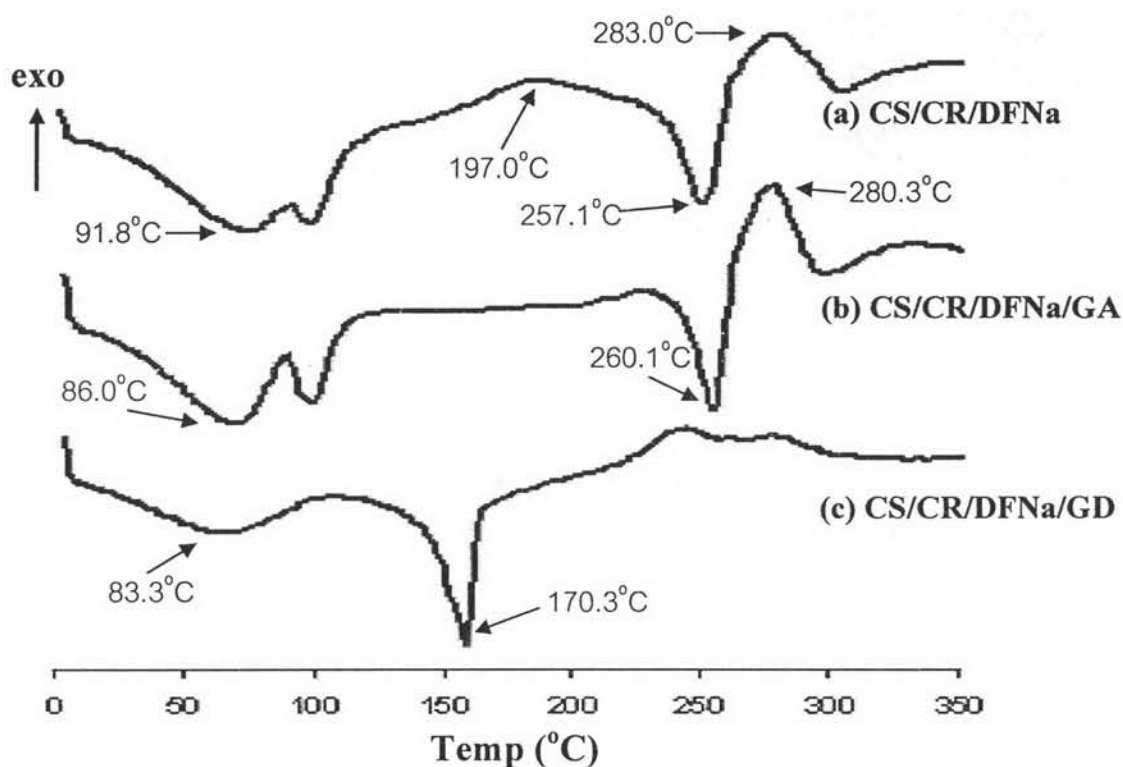


Figure 4.16 DSC thermograms of (a) CS/CR/DFNa, (b) CS/CR/DFNa/GA and (c) CS/CR/DFNa/GD bead.

The effects of cross-linking agents on the thermal behavior of the beads were shown in Figure 4.16. The non-crosslinked bead and the glutaric acid-crosslinked bead showed substantially no difference in its DSC thermogram pattern, except that the exothermic peak of the polymer bead at 197.0°C disappeared. This indicated that there was an anionic interaction between chitosan

and glutaric acid. The bead crosslinked with glutaraldehyde on the other hand, showed a different DSC pattern with a broad endothermic peak at 83.3°C and a new endothermic peak at 170.3°C. The decomposition peaks of both polymer and DFNa disappeared. The results indicated that the chemical interaction between glutaraldehyde and the compositions inside the bead was relatively strong resulting in the absence of the decomposition peak for both polymer and drug at higher temperature.

4.2.3.2 Thermogravimetric analysis (TGA)

The composition and the weight change of sample were analyzed by thermogravimetric analysis (TGA). The TG curves recorded the weight change (%) of sample as a function of temperature (°C). Then, the derivative thermogravimetric (DTG) curve which is the first derivative of the weight change of the sample as a function of temperature with respect to time (dm/dt) was obtained. The TG and DTG curves of samples are shown in Figure 4.17 and 4.18. The TGA data of the samples are shown in Table 4.3.

The TG curve of the pure chitosan bead, Figure 4.17 (a), shows a weight loss of about 21.85% in the temperature range from 40.0 to 153.0°C. This may be the result of the loss of water in the beads. This implies that chitosan is a good moisture absorber. Furthermore, the weights of the chitosan beads decrease continuously in the temperature range from 157.0 to 550.0°C with an additional DTG peak at 191.0°C, presumably due to the degradation of the chitosan. The degradation of the pure carrageenan beads occurred in two stages in the TG curve (Figure 4.17 (b)). The first stage, in the temperature range from 35.0 to 200°C, showed a water loss of about 9.43%. The second stage, in temperature range from 200.0 to 550.0°C with an additional peak of the DTG at 258.0°C, is due to the degradation of carrageenan.

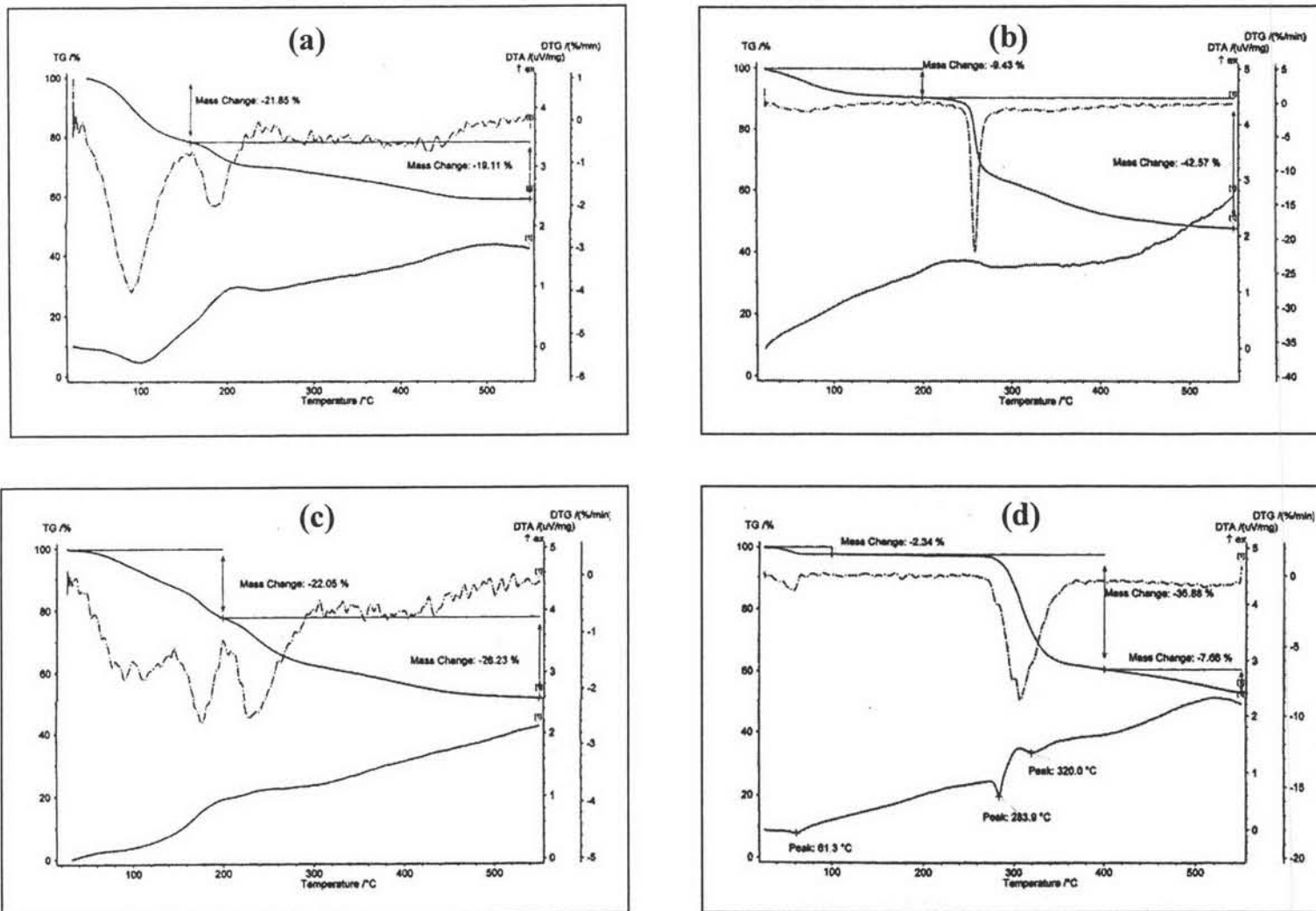


Figure 4.17 TGA and DTG curves of (a) pure chitosan (CS), (b) pure carrageenan (CR), (c) CS/CR bead, and (d) DFNa.

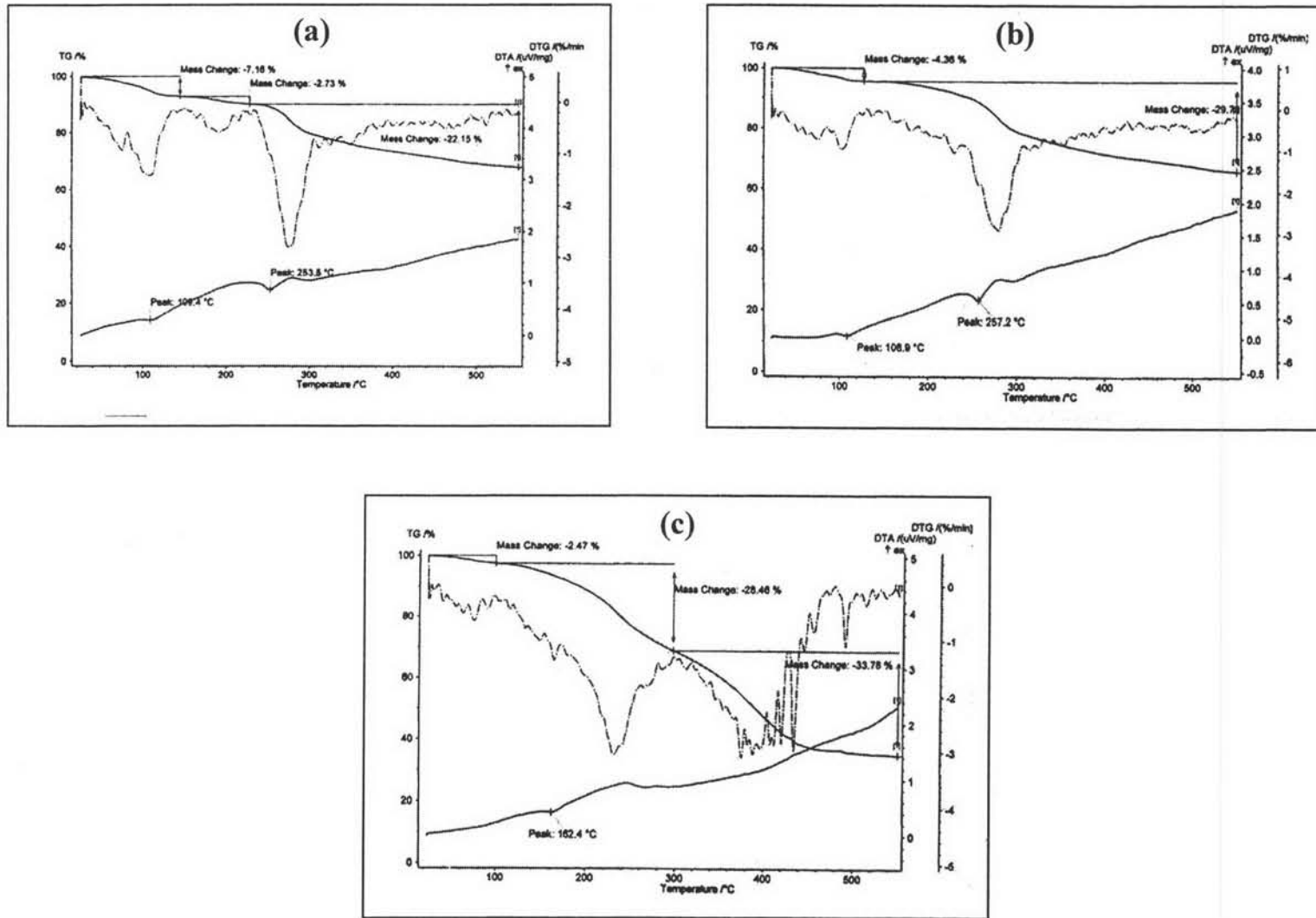


Figure 4.18 TGA and DTG curves of (a) CS/CR/DFNa, (b) CS/CR/DFNa/GA, and (c) CS/CR/DFNa/GD bead.

Table 4.3 Thermogravimetric analysis of the substances and the beads obtained by various compositions

Composition	Temp. range (°C)	Weight loss (%)	DTG peak (°C)
pure CS Bead	40.0 - 153.0	21.85	91.0
	157.0 - 550.0	19.11	191.0
pure CR bead	35.0 - 220.0	9.43	74.0
	200.0 - 550.0	42.57	258.0
CS/CR (Formulation H)	40.0 - 201.0	22.05	177.0
	201.0 - 550.0	26.23	231.0
DFNa	35.0 - 97.0	2.34	58.0
	220.0 - 550.0	44.54	306.0
CS/CR/DFNa (Formulation L)	40.0 - 130.0	7.16	110.0
	130.0 - 232.0	2.73	194.0
	232.0 - 550.0	22.15	278.0
CS/CR/DFNa/GA (Formulation O)	40.0 - 134.0	4.36	106.0
	134.0 - 550.0	29.79	280.0
CS/CR/DFNa/GD (Formulation S)	40.0 - 113.0	2.47	75.0
	113.0 - 281.0	28.46	233.0
	281.0 - 550.0	33.78	375.0

The thermogravimetric analysis of chitosan/carrageenan (CS/CR:2/1) bead (Formulation H) was shown in Figure 4.17 (c). It showed a continuous weight loss from 40.0 to 550.0°C. The initial weight loss is due to the evaporation of water inside the beads. The weight loss at higher temperature is due to the decomposition of the polymer bead. The DTG peak of chitosan and carrageenan showed a decreasing temperature from 191.0 to 177.0°C and from 258.0 to 231.0°C, respectively. This may be attributed to the fact that chitosan and carrageenan existed in the PEC form and the thermal stability of PEC was less than that of the chitosan and carrageenan alone.

The degradation of DFNa occurred in two stages (Figure 4.17 (d)). The first stage showed a small weight loss of about 2.34% in the temperature range from 35.0 to 97.0°C due to the loss of water while the second stage showed a weight loss from 220.0 to 550.0°C, with a peak in the first derivative at 306.0°C, probably due to the decomposition of DFNa. The TG curve of the DFNa-loaded chitosan/carrageenan (CS/CR: 2/1) bead with 5% (w/v) DFNa content (Formulation L) was shown in Figure 4.18 (a). This curve indicates that the combination of polymer and drug had three degradation stages. The first stage, the weight loss of about 7.16% in temperature range from 40.0 to 130.0°C is due to the loss of water. In the second stage, the weight loss of about 2.73% in the temperature range from 130.0 to 232.0°C, was due to the degradation of the polymer bead. The third stage in the temperature range from 232.0 to 550.0°C, with a peak in the first derivative at 278.0°C was due to the degradation of DFNa together with the polymer bead. The different decreasing slope of TG curve indicated that there was no interaction between the polymer bead and the drug.

The TG curve of the chitosan/carrageenan (CS/CR : 2/1) bead with 5% DFNa and crosslinked with 0.25% glutaric acid (Formulation O) was shown in Figure 4.18 (b). Unlike the non-crosslinked bead, this curve exhibits no DTG peak of polymer bead at 194.0°C. This result indicated that there were interactions between chitosan and glutaric acid which cause a slight increase in the temperature of the polymer bead together with the degradation stage of DFNa in temperature range from 134.0 to 550.0°C (DTG peak at 280.0°C).

The degradation of the chiosan/carrageenan (CS/CR : 2/1) with 5%DFNa crosslinked with 5.00% glutaraldehyde (Formulation S) was shown in the TG curve, Figure 4.18 (c). It shows a continuous weight loss from 40.0 to 550.0°C. The initial weight loss of about 2.47% in temperature range from 40.0 to 113.0°C is due to the water loss. The weight loss in temperature range from 113.0-281.0°C and 281.0 to 550.0°C were due to the decomposition of the drug and the polymer, respectively. This indicates the interaction between glutaraldehyde and

chitosan which cause the increase of temperature of the decomposition of the polymer bead.

4.3 The Encapsulation Efficiency of The Beads

The encapsulation efficiency (%EE) of the DFNa-loaded beads prepared from various compositions are shown in Table 4.4. The values of %EE from these beads were in the range of 65% to 97% depending on the compositions of the formulations. The highest %EE was obtained from Formulation I (96.91%) and the lowest %EE was obtained from Formulation S (65.36%). Formulation A to G showed the effect of chitosan/carrageenan ratio on the %EE of the beads. The %EE of the chitosan/carrageenan beads (84.69-89.70%) was higher than that of the pure chitosan bead (Formulation A, 79.59%). The results may be due to the $-\text{SO}_4^{2-}$ groups of carrageenan which electrostatically interacted with the $-\text{NH}_3^+$ groups of chitosan in the polyelectrolyte complex (PEC) form, thus, the drug was more favorably entrapped into the PEC form of the chitosan/carrageenan bead than the pure chitosan bead. As for Formulation E-G, the %EE of the beads could not be determined because the obtained beads were fragile and were not well formed and hence broken into pieces after drying.

The %EE of the DFNa-loaded beads at different DFNa contents (1-5% (w/v)) were studied in Formulation C, I, J, K and L. The %EE increased from 84.69% to 96.91% as the DFNa content was increased from 1% to 2% (w/v). Presumably, the drug was entrapped more efficiently in the viscous hydrogel resulting from the higher drug content. However, when the drug content was increased from 2% to 3-5% (w/v), the %EE decreased from 96.91% to 76.38-89.30%. This is because there were too much drug to be entrapped into the beads.

Table 4.4 The encapsulation efficiency (%EE) of the formulated beads with various compositions

Formulation	CS/CR ratio	DFNa Content (%W/V)	Crosslinking agent		%EE ± S.D.
			(%W/V)		
			GA	GD	
A	1/0	1	-	-	79.59±1.56
B	3/1	1	-	-	89.70±0.71
C	2/1	1	-	-	84.69±1.96
D	1/1	1	-	-	89.19±0.31
E	1/2	1	-	-	- ^a
F	1/3	1	-	-	- ^a
G	0/1	1	-	-	- ^a
H	2/1	-	-	-	- ^b
I	2/1	2	-	-	96.91±1.86
J	2/1	3	-	-	76.38±3.53
K	2/1	4	-	-	84.80±4.30
L	2/1	5	-	-	81.83±5.59
M	2/1	5	1.00	-	- ^a
N	2/1	5	-	1.00	- ^a
O	2/1	5	0.25	-	90.30±0.17
P	2/1	5	0.50	-	84.01±1.39
Q	2/1	5	0.75	-	91.99±1.45
R	2/1	5	1.00	-	93.64±0.73
S	2/1	5	-	5.00	65.36±2.51

^a The %EE could not be determined because the beads were not successfully prepared.

^b The beads without DFNa.

The effects of crosslinking agent concentrations on the %EE were illustrated in the Formulation M to S. The %EE of beads from Formulation M to N could not be determined because of the high viscosity of the hydrogel solution. The %EE of the crosslinked beads with glutaric acid at 0.25-1.00% (w/v) (84.01-93.64%) were higher than that of the non-crosslinked bead (81.83%). This high %EE is likely the result of the formulation of strong ionic crosslink between glutaric acid and chitosan.

As for the glutaraldehyde crosslinked bead, the %EE (65.36%) was less than that of the non-crosslinked bead (81.83%). This is because glutaraldehyde formed a covalent crosslink with chitosan. This consequently made the bead more rigid and decreased the free volume space within the bead, thus reducing the %EE.

4.4 Swelling Study

The swelling behavior study of the bead was performed in three dissolution systems, (i) 0.1N HCl (pH 1.2), (ii) phosphate buffer saline pH 7.4 and (iii) the pH-alternating system. In the pH-alternating system, the bead was immersed in 0.1N HCl for the first 2 hours, then, transferred to the phosphate buffer saline pH 7.4 and immersed for another 5 hours. The chitosan/carrageenan (CS/CR : 2:1) bead with 5% (w/v) DFNa content was selected for this study because it showed the optimum DFNa release profile.

The swelling ratios of the bead in different dissolution systems as a function of time are shown in Figure 4.19 (see Table B1, Appendix B). The swelling ratios of the bead in 0.1N HCl (pH 1.2), phosphate buffer saline pH 7.4 and the pH-alternating system were not significantly changed. After 30 minutes in the pH 1.2 system, the swelling ratio of this bead was 0.95, indicating that the bead shrank slightly. The shrinking of the bead may be the result of the ionic interactions between the $-\text{NH}_3^+$ groups of chitosan and the $-\text{SO}_4^{2-}$ groups of carrageenan forming a strong PEC. The swelling ratio of the bead in the dissolution medium pH 7.4 slightly increased in the first hour but did not change when the time increased afterward. In the pH-alternating system, the bead was not significantly swelled. Overall, there was no significant swelling of the bead after immersing in all the test dissolution systems.

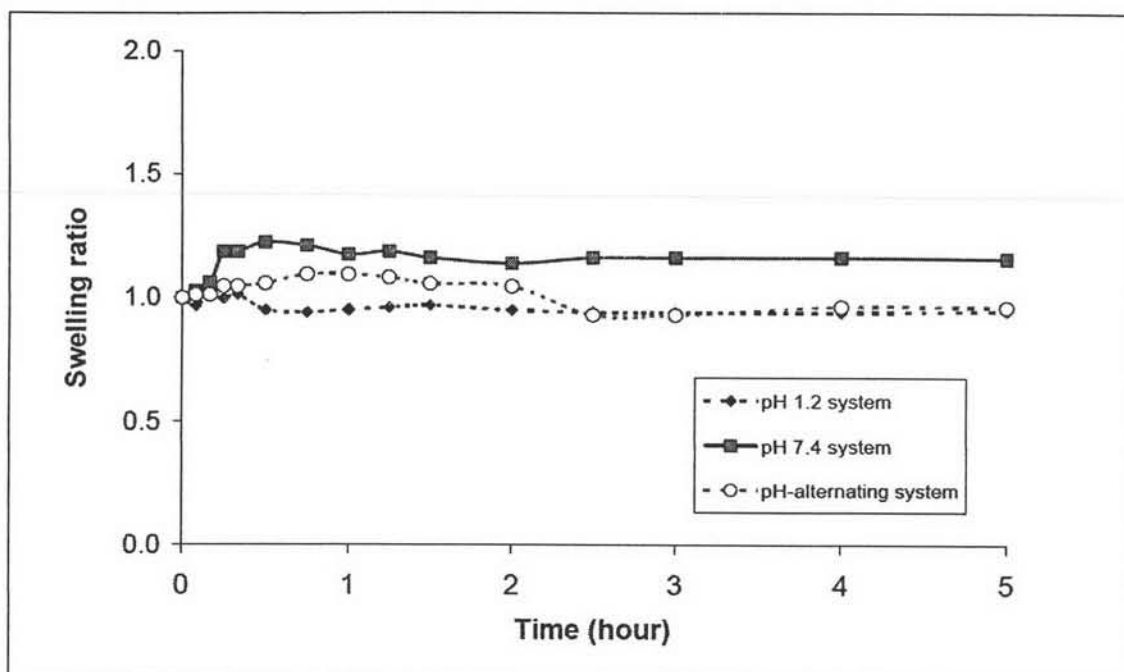


Figure 4.19 Swelling behavior of the chitosan/carrageenan (CS/CR : 2/1) bead with 5% (w/v) DFNa content in the three dissolution systems; (i) pH 1.2 system, (ii) pH 7.4 system and (iii) pH-alternating system.

Figure 4.20 shows the photographs of the chitosan/carrageenan (CS/CR : 2/1) bead with 5% (w/v) DFNa and the bead after the swelling test in the three dissolution systems. The beads were not swollen and showed no erosion. This may be the result of the electrostatic interaction between functional groups of chitosan and carrageenan in the dissolution medium pH 1.2 and pH 7.4. Our results agree with Sakiyama et al. ^[7] who reported that the swelling of chitosan and carrageenan gel was not observed at pH below 9.

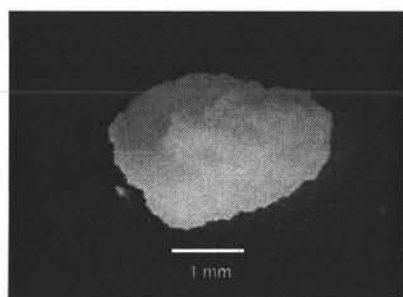
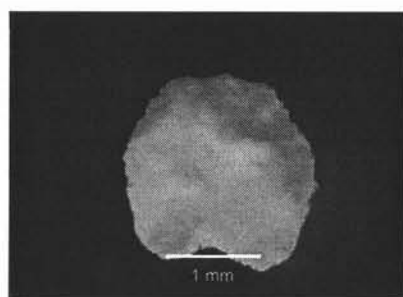
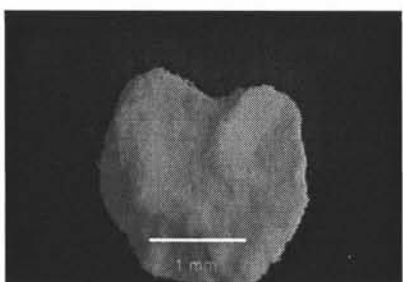
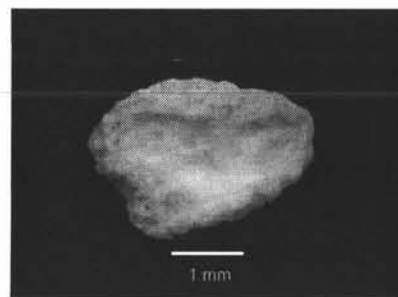
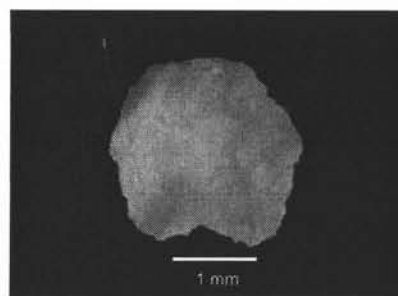
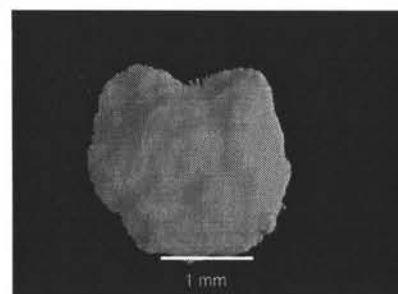
Dried bead before swelling test**(a) pH 1.2 system****(b) pH 7.4 system****(c) pH-alternating system****Bead after swelling test for 5 hrs****(a) pH 1.2 system****(b) pH 7.4 system****(c) pH-alternating system**

Figure 4.20 Photomicrographs of the chitosan/carrageenan (CS/CR : 2/1) bead with 5% (w/v) DFNa and the bead after swelling test in the three dissolution systems; (a) pH 1.2 (b) pH 7.4 and (c) pH-alternating system, (x 4).

A possible swelling mechanism for the gel bead is illustrated in Figure 4.21. The bead prepared in this study contained both the $-\text{SO}_4^{2-}$ groups of carrageenan and the $-\text{NH}_3^+$ groups of chitosan. In the acid dissolution, these two functional groups are considered to be oppositely charged and thus electrostatically bound to each other. In alkaline dissolution, the $-\text{NH}_3^+$ groups will be neutralized, and the $-\text{SO}_4^{2-}$ groups will remain negatively charge. Therefore, the electrostatic linkage between the two functional groups will diminish, and the electrostatic repulsion between $-\text{SO}_4^{2-}$ groups will contribute to the swelling of gel.

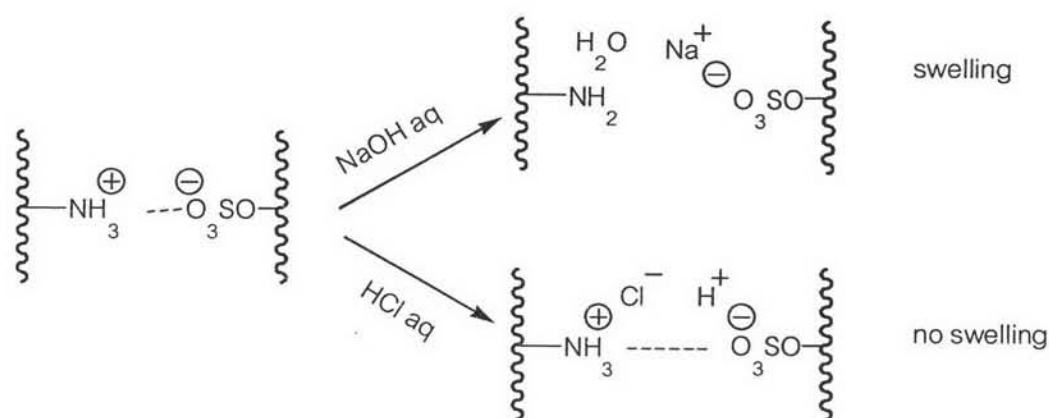


Figure 4.21 Swelling mechanism of the chitosan/carrageenan gel ^[7].

The beads were not swollen nor eroded in all three dissolution systems. Therefore, the drug release was not the effect of the swelling of the bead but was likely controlled by the dissolution of DFNa in the dissolution medium and the diffusion of DFNa through polymer matrix.

4.5 In Vitro Release Study

4.5.1 Dissolution profiles and release rate profiles

The dissolution profiles can be illustrated by a plot of the amounts of drug release versus time. Changes in the rate of drug release were constructed from the dissolution profile to elucidate the release rate at various time intervals during the course of drug dissolution from the beads. The dissolution and release rate data of each formulation are given in Table C1-C2 (Appendix C).

The release rate was calculated by dividing the difference of percent drug release at various time intervals with the time utilized to release that certain amount of drug. It was shown that the rate of release decreased with time.

The release studies of DFNa from the commercial products and formulation A to S (see compositions Table 3.2, Chapter 3) were evaluated in 0.1N HCl (pH 1.2), phosphate buffer saline pH 6.6, and pH 7.4 by pH-alternating method. These dissolution profiles and release rate profiles are shown in Figure 4.23-4.26 and 4.28-4.31. In the pH-alternating system, the beads were tested in acidic condition (0.1N HCl, pH 1.2) for 2 hours. The percentage of drug release from formulations A to D were less than 15% while those of formulations I to L and O to R were less than 5%, and less than 1.5% for formulations S. When the dissolution medium was changed to phosphate buffer saline pH 6.6 for 1 hour, their percentage increased slightly. Then, the beads were subjected to the phosphate buffer saline pH 7.4 and were continuously tested up to 24 hours. In this solution, the drug release from all formulations increased rapidly. The results indicated that the release of DFNa from the beads strongly depend on pH of the dissolution medium. DFNa is an acid addition salt (Monosodium-2-(2,6-dichloroanilino)phenylacetate), therefore, the solubility is strongly dependent to the ionization constant (K_a), and the pH of the dissolution medium ^[46]. In acidic solution, DFNa was neutralized by hydrogen ion and converted to diclofenac acid

(DFH) (Figure 4.22), which had lower solubility and become precipitated in the matrix ^[47].

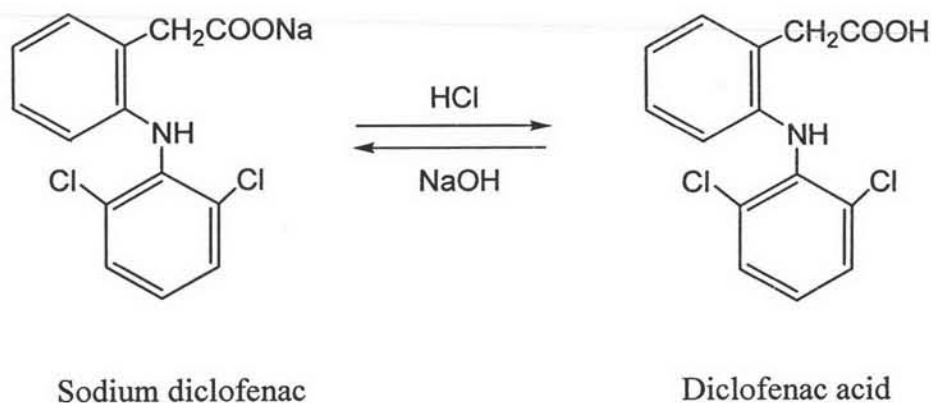


Figure 4.22 Chemical structures of sodium diclofenac and diclofenac acid.

4.5.1.1 The dissolution profiles of the commercial diclofenac sodium product

The commercial products used were Voltaren[®] SR tablets (as 25 mg) and Subsyde[®] CR capsules (as 100 mg).

(1) The Voltaren[®] SR tablet

The drug release data of Voltaren[®] SR tablet in the pH-alternating system is listed in Table C1-C2 (Appendix C). The dissolution profile of DFNa from Voltaren[®] SR in the pH-alternating system is shown in Figure 4.23. In the first 3 hours (pH 1.2 and 6.6), the average percentage of drug release was less than 0.5%. By the fourth hour, in phosphate buffer saline pH 7.4, the drug was completely dissolved because the enteric coat of the tablet was dissolved and cracked. The release rate increased rapidly upon immersed in this solution and then decreased slightly as the time increased (Figure 4.24).

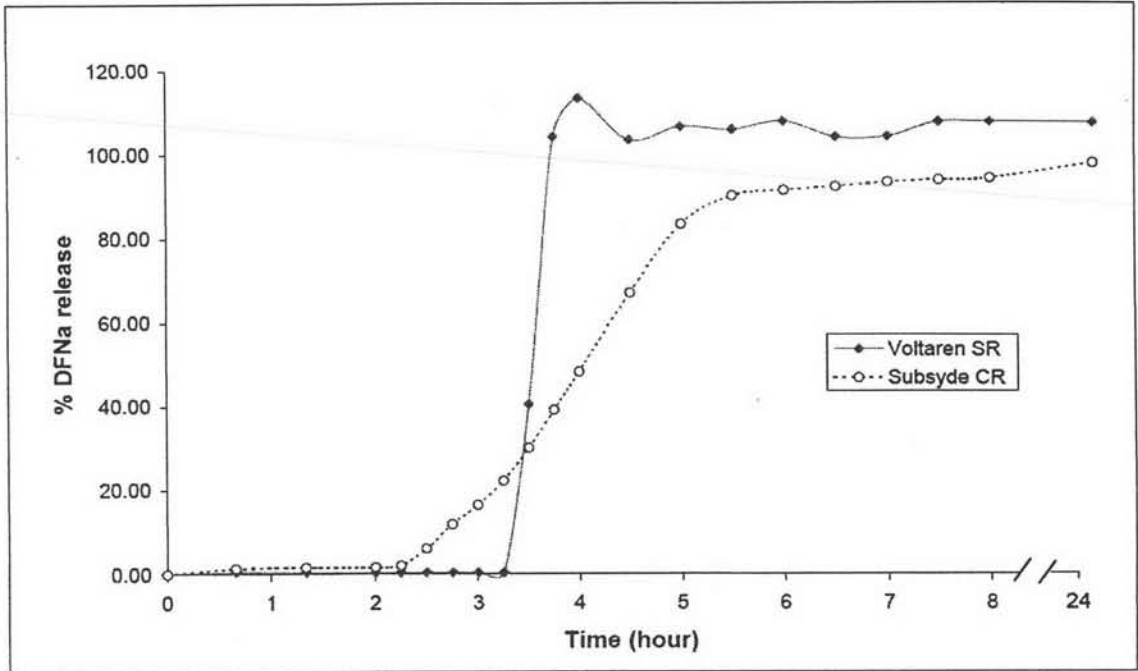


Figure 4.23 The dissolution profiles of sodium diclofenac from the commercial products in the pH-alternating system.

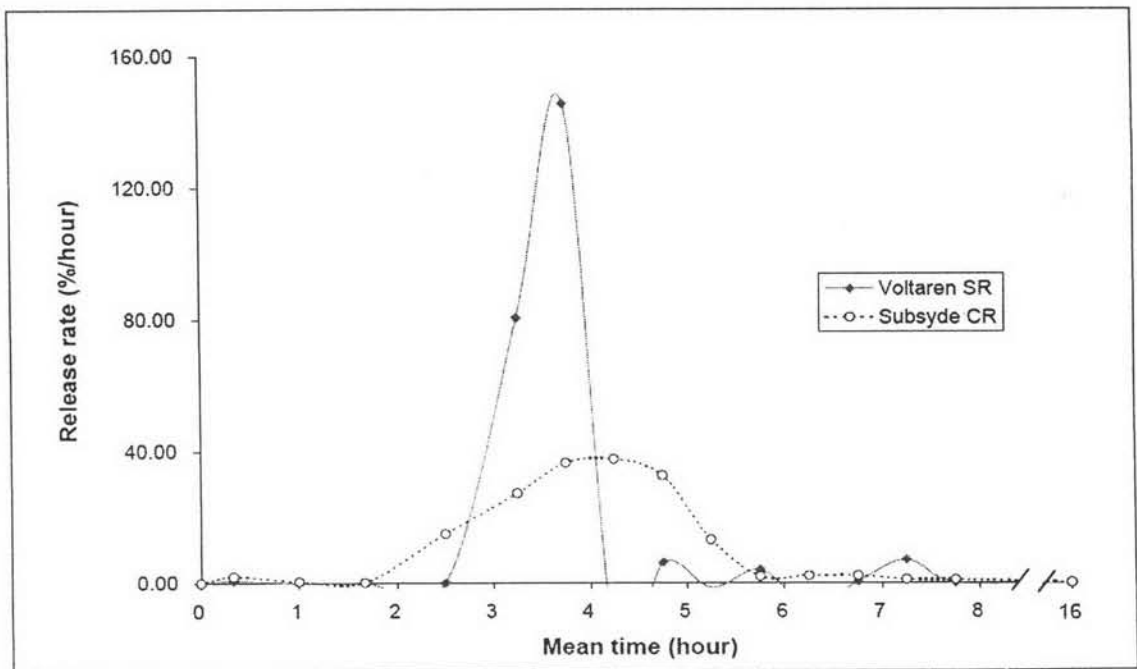


Figure 4.24 The release rate profiles of sodium diclofenac from the commercial products in the pH-alternating system.

(2) The Subsyde[®] CR capsule

Approximately 1/4 of the capsule from the Subsyde[®] CR capsule (about 25 mg) were evaluated in the pH-alternating system. The amounts of drug release at specific time intervals and release rate data are presented in Table C1-C2 (Appendix C). The dissolution profile and the release rate profile of DFNa from the Subsyde[®] CR capsule were affected by the release dissolution medium as illustrated in Figure 4.23 and 4.24. In the pH-alternating system, the drug release from the Subsyde[®] CR capsule was less than 2% in the first 2 hours (pH 1.2) and was less than 17 % in the phosphate buffer saline pH 6.6. The drug release was more than 80% within the fifth hour in the phosphate buffer saline pH 7.4. After 24 hours, the percentage of drug released was increased to 98.13% while the beads were still in the original shape and with no erosion.

4.5.1.2 Effect of polymer ratios on the dissolution profiles

The dissolution profiles of DFNa from the beads with various chitosan/carrageenan (CS/CR) ratios (Formulation A to G, see Table 3.2, Chapter 3) in 0.1N HCl, phosphate buffer pH 6.6 and pH 7.4 using pH-alternating method are shown in Figure 4.25. (Table C1, Appendix C). Each point represents the average value obtained from three determinations at each sampling time. The release pattern strongly depended on pH of the release dissolution medium. The release rate decreased with time as shown in Figure 4.26 (Table C2, Appendix C).

In the pH-alternating system, in the first 2 hours (pH 1.2), the average drug release from the chitosan/carrageenan ratios of 1/0, 3/1, 2/1 and 1/1 (Formulation A to D) were less than 15% and slightly increased to 16-18% in the third hour (pH 6.6). After the beads were subjected to the release dissolution medium pH 7.4, the DFNa release at 24 hours were 52.98% and 52.86% for chitosan/carrageenan ratio of 1/0 and 3/1, respectively.

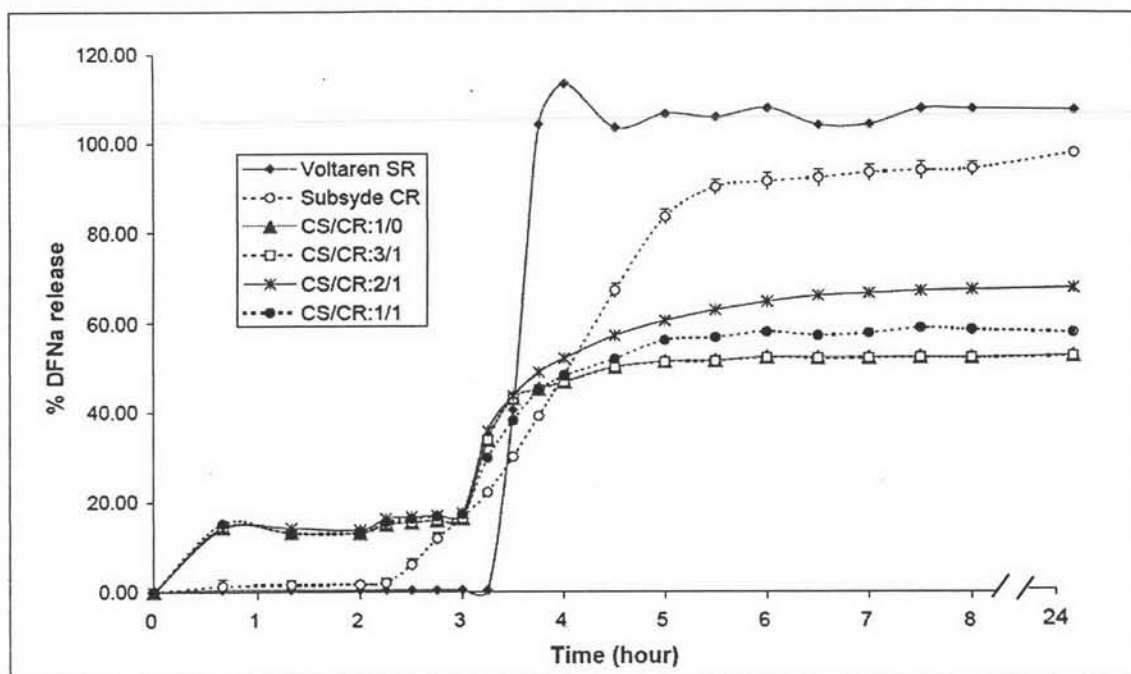


Figure 4.25 The dissolution profiles of sodium diclofenac from the beads with various chitosan/carrageenan (CS/CR) ratios in the pH-alternating system.

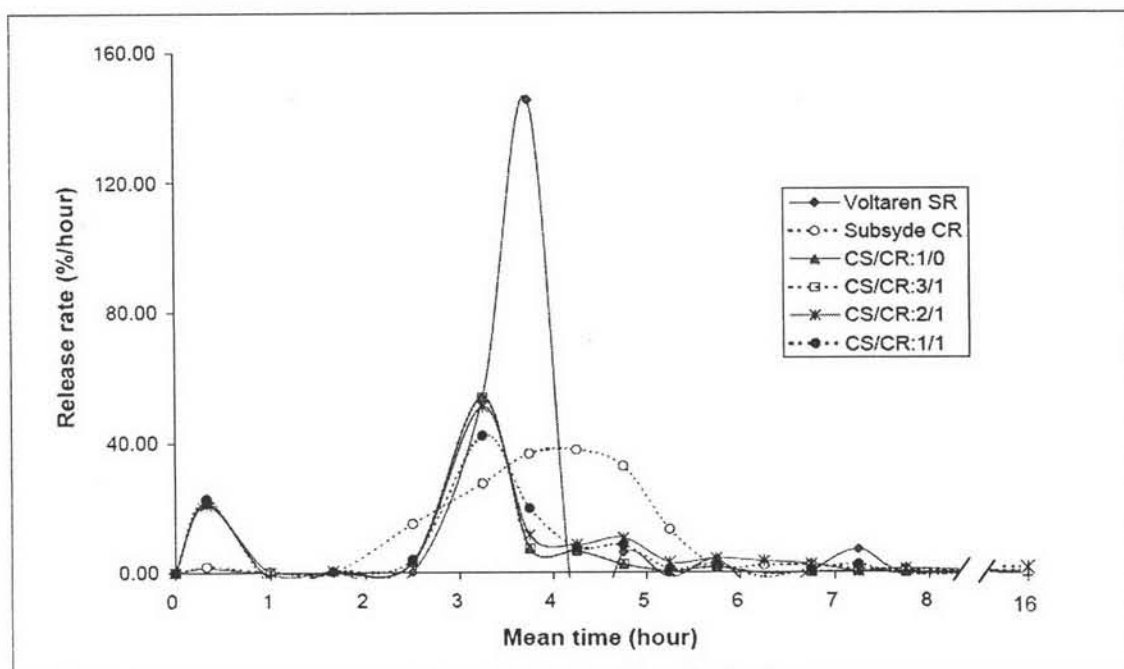


Figure 4.26 The release rate profiles of sodium diclofenac from the beads with various chitosan/carrageenan (CS/CR) ratios in the pH-alternating system.

These formulations showed no difference in the drug release pattern. When the proportions of carrageenan in the formulations increased from the chitosan/carrageenan ratio of 3/1 to 2/1 and 1/1, the DFNa release in the twenty-fourth hour increased from 52.86% to 68.07% and 58.16%, respectively. This indicates that the drug release increase with the increasing amount of carrageenan in the formulations. Carrageenan is a hydrophilic polymer which promotes the entry of the release dissolution into the beads. Therefore, it greatly improves the solubility of the drug and accelerates the dissolution. As for the formulation prepared by using the chitosan/carrageenan ratio of 1/1, the DFNa release at the twenty-fourth hour was less than that of the chitosan/carrageenan ratio of 2/1. The reason for this lies in the differences in the electrostatic interaction within the beads which help controlled the drug release.

The dissolution profiles of DFNa from the chitosan/carrageenan ratios of 1/2, 1/3 and 0/1 were not studied (Formulation E to G), due to the gelling property of carrageenan at room temperature. When the proportions of carrageenan in the hydrogel solution increased, the solution become more viscous and, made it difficult to drop into a bead form. Moreover, carrageenan attracts a lot of water content into the beads and cause the beads to be easily destroyed after the filtering and washing, and broken into pieces after drying.

Hence, the chitosan/carrageenan ratio of 2/1 was chosen for the bead preparation in the following studies because it showed optimal release profile along with minimum drug and bead losses.

4.5.1.3 Effect of the drug contents on the dissolution profiles

The chitosan/carrageenan ratio of 2/1 was used for the formulations of the beads with various DFNa content (1-5 % (w/v)), in Formulation C, I, J, K and L (see Table 3.2, Chapter 3). The dissolution and release rate data and the dissolution profiles of DFNa from these formulations in the pH-alternating system are given in Table C1-C2 (Appendix C), and Figure 4.28. The results revealed that the release profiles of the beads strongly depended on the pH of dissolution medium.

In the pH-alternating system, at pH 1.2, the drug release from Voltaren[®] SR tablet was negligible (less than 0.5%). Meanwhile, the drug release from Formulation I to L, were approximately 5-7% and were not changed until 2 hours. This early drug release might be coming from the unencapsulated drug (Figure 4.27). For Formulation C, the beads with 1% (w/v) DFNa, the drug release in the dissolution medium pH 1.2 increased to 14%. This is probably because the drug was less encapsulated than the other formulations, as can be seen from %EE of 84.69%.

After immersion in the pH 1.2 system for 2 hours, the dissolution medium was changed to phosphate buffer saline pH 6.6, the drug still dissolved into the dissolution medium, therefore, the percentages of drug release were slightly increased to 6-9% for Formulations I to L, and to 17% for Formulation C.

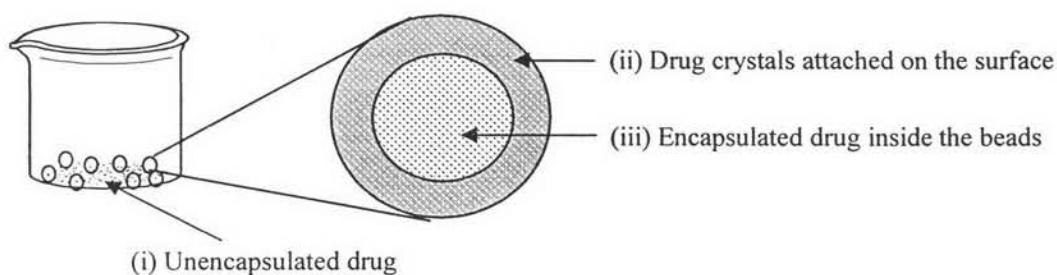


Figure 4.27 Schematic representation of the drug in the bead.

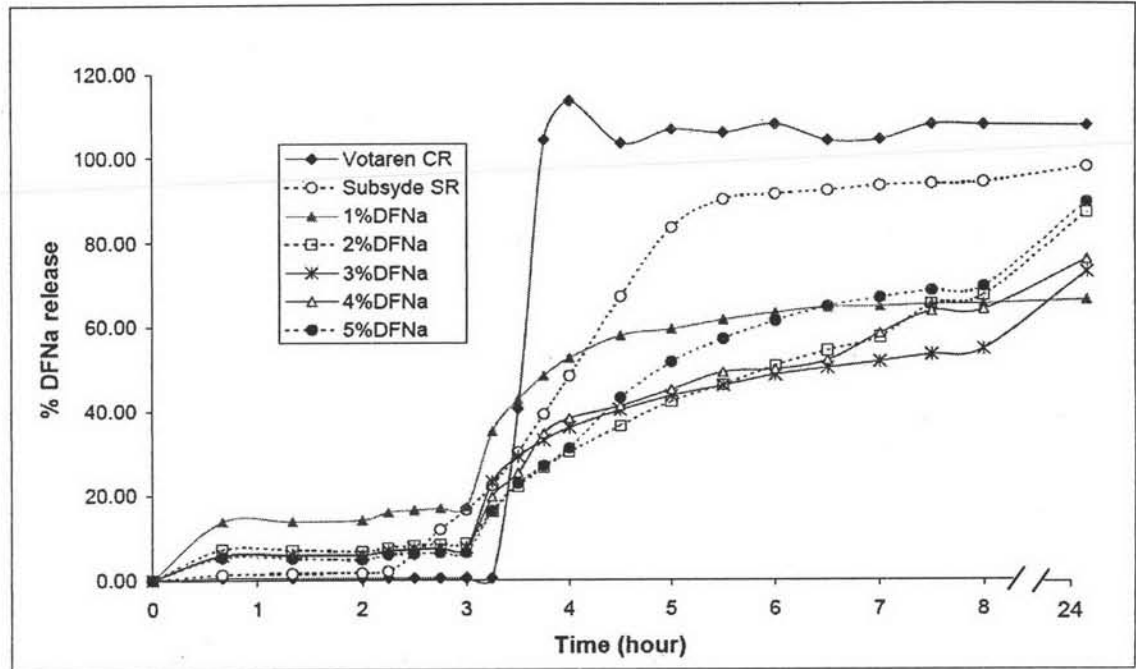


Figure 4.28 The dissolution profiles of sodium diclofenac from the chitosan/carrageenan (CS/CR : 2/1) beads with various drug content (%w/v) in the pH-alternating system.

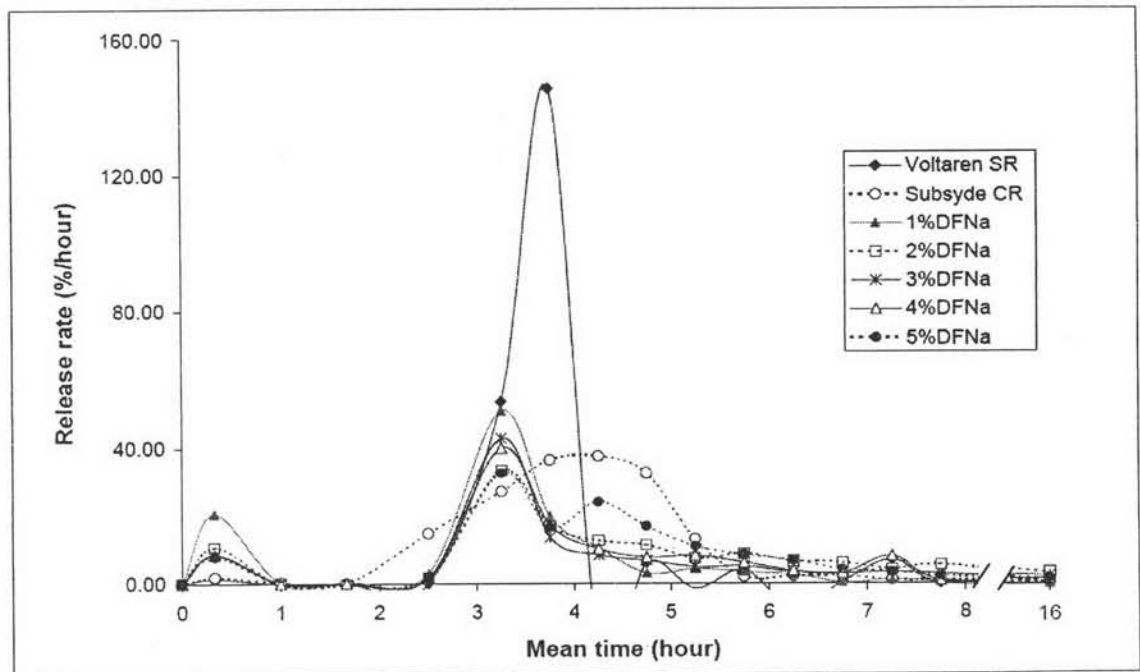


Figure 4.29 The release rate profiles of sodium diclofenac from the chitosan/carrageenan (CS/CR : 2/1) beads with various drug content (%w/v) in the pH-alternating system.

In the phosphate buffer saline pH 7.4, the drug release profiles could be explained by two mechanisms, (i) the dissolution of the drug from the surface and (ii) the diffusion of the drug through the hydrogel bead. In the first hour in this solution, the drug release rapidly increased because of the high solubility of DFNa, which was only attached to the surface of the beads.

After the first hour in this solution, the drug release increased slowly as most of the drug release occurred via the diffusion of drug through the bead.

At the twenty-fourth hour, the percentages of DFNa release were 68.07%, 77.33% and 76.27% for Formulation C, J and K and more than 85% for Formulation I and L, respectively. This indicated that the diffusion of drug through the hydrogel bead was not complete because the polymer chains in the beads were entangled together with the strong ionic interactions between the two polymers. Thus, the penetration of the dissolution medium into the hydrogel bead became more difficult.

The release rate profiles of these formulations (Formulation C, I, J, K and L) were shown in Figure 4.29. The release rate of Voltaren[®] SR tablet was very high during the third - the fourth hour and rapidly decreased thereafter. Meanwhile, the release rate of the beads from Formulation C and I, J, K and L were lower and slowly decreased at the same time. Especially, Formulation L showed the slowest decrease of the drug release rate. This implied that the drug released from the beads can be maintained for a long period of time. As a result, the beads from Formulation L, the bead with 5% (w/v) DFNa content, showed potential to be a better drug prolonged release carrier than the other formulations.

4.5.1.4 Effect of cross-linking agents on the dissolution profiles

Glutaric acid is an anionic cross-linking agent. It has the COOH groups, which can convert to the COO⁻ groups. The COO⁻ groups are able to interact with the -NH₃⁺ of chitosan, depending on the pH of the dissolution medium and the glutaric acid concentration. The interaction affects the release of drug from the bead by prolonging the drug release period. Another chemical, glutaraldehyde, was used for cross-linking as it has carbonyl groups which is able to covalently crosslink with amine groups of chitosan.

The dissolution profiles from the previous section indicated that the chitosan/carrageenan ratio of 2/1 with 5% (w/v) DFNa content yield the best result; therefore, it was selected as the beads model in this study. The preparation were carried out in similar manner, except that the beads were crosslinked with various concentrations of glutaric acid, 0.25-1.00% (w/v) (Formulation O to R), and glutaraldehyde at 5.00% (w/v) (Formulation S). The dissolution profiles and the release rate profiles of DFNa from the beads with various concentrations of cross-linking agent in the pH-alternating system are shown in Figure 4.30 and 4.31. The amounts of drug release at specific time interval and release rate data are presented in Table C1-C2 (Appendix C).

The beads crosslinked with glutaric acid at different concentrations (0.25-1.00% (w/v)) showed no difference in the drug release pattern. In the pH-alternating system, in the first 2 hours (pH 1.2), the DFNa release from the beads were less than 5%. When the pH of the dissolution medium was raised to 6.6, the amounts of drug release slightly increased to 6-14%. Next, the beads were subjected to phosphate buffer saline pH 7.4. The drug release was increased to 50-58% at 24 hours.

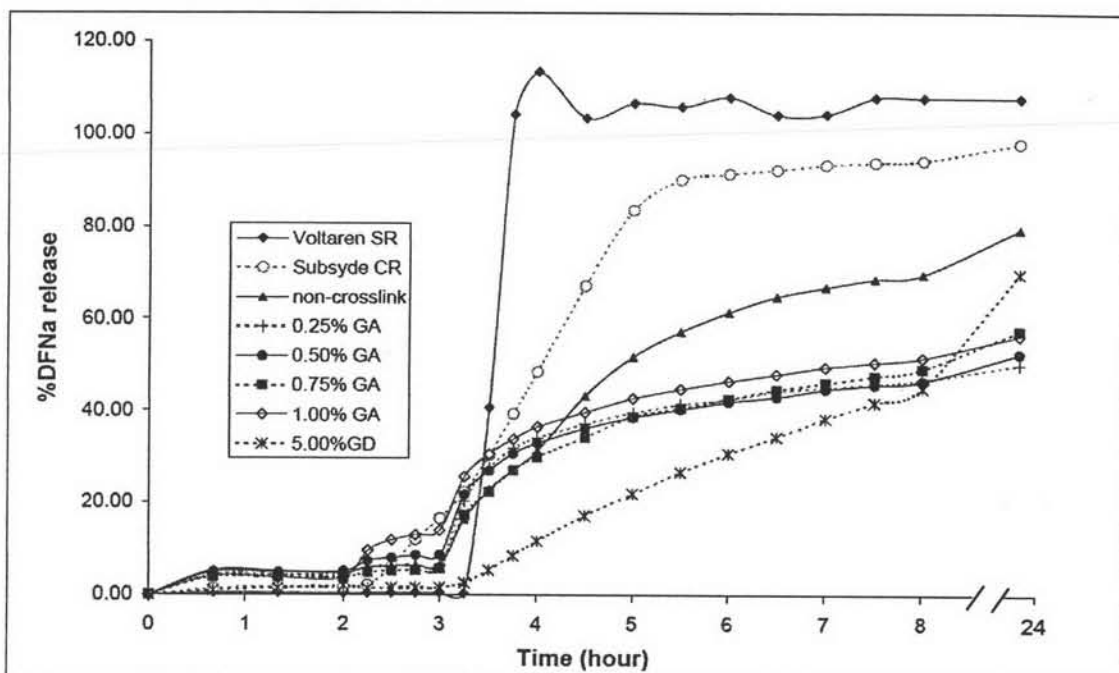


Figure 4.30 The dissolution profiles of sodium diclofenac from the chitosan/carrageenan (CS/CR : 2/1) beads with 5%(w/v) DFNa content prepared at different concentration of cross-linking agent in the pH-alternating system.

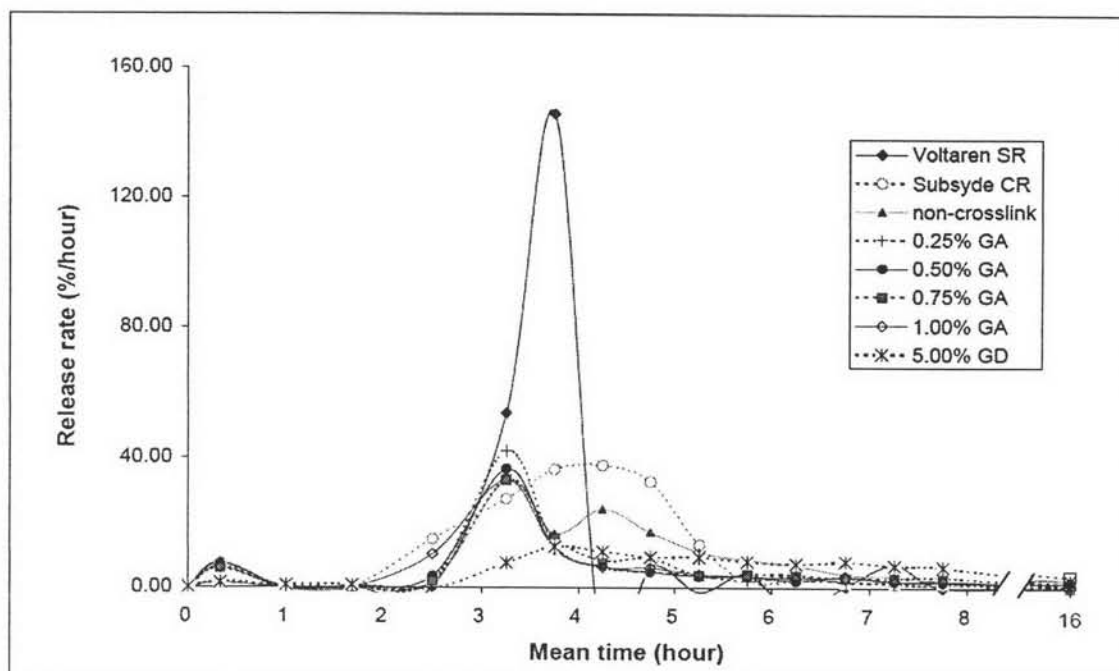


Figure 4.31 The release rate profiles of sodium diclofenac from the chitosan/carrageenan (CS/CR : 2/1) beads with 5%(w/v) DFNa content prepared at different concentration of cross-linking agent in the pH-alternating system.

Upon comparing the dissolution profiles of the glutaric acid-crosslinked beads with the non-crosslinked bead, it was found that the amount of drug released from the crosslinked beads (Formulation O to R) were lower than that of the non-crosslinked bead (Formulation L) in the dissolution medium pH 7.4., indicating that there were interactions between the -NH_3^+ groups of chitosan and the -COO^- groups of glutaric acid. This interaction makes it difficult for the dissolution medium to penetrate into the hydrogel beads. Therefore, the dissolution and the diffusion of drug through the hydrogel beads were less than that of the non-crosslinked beads.

The drug release of the beads crosslinked with 5.00% (w/v) glutaraldehyde (Formulation S) was less than 2% in the first 3 hours (pH 1.2 and pH 6.6). When the pH of the dissolution medium was increased to pH 7.4, the drug release increased continuously and reached 69.98% at the twenty-fourth hour. The release rate of this formulation was the slowest of all formulations and, therefore, was able to extend the drug release for a longer period. This is very beneficial for maintaining the drug concentration in the therapeutic range. As a result, it can be concluded that the crosslinked bead with glutaraldehyde showed the best result as a prolonged release carrier.

4.5.2 Drug release models

To study the drug release kinetics of the investigated beads, analysis of all dissolution profiles was fitted to the zero-order, the first-order and Higuchi's square root time model. For the zero-order model ($Q = k_0t$), the graph was plotted as percentage of drug release (Q) versus time (t), where k_0 = the zero-order constant. In the first-order model ($\ln A_t = \ln A_0 - k_1t$), the graph was plotted as log percentage of drug remained ($\ln A_t$) versus time (t), where A_0 = the initial amount of drug in the beads, and k_1 = the first-order constant. Finally, for the Higuchi model ($Q = k_h t^{1/2}$), the graph was plotted as percentage of drug release (Q) versus square root of time ($t^{1/2}$), where k_h = Higuchi constant.

The correlation coefficient statistics were used to determine the most appropriate model. The best fitted model is indicated by the one with the correlation coefficient closest to 1.

From the dissolution profiles of all formulations, the release of drug was evaluated in the three dissolution media (pH 1.2, 6.6 and 7.4) by the pH-alternating method. The analysis of drug release model was performed by fitting the plots to the zero-order, the first-order, and the Higuchi model. The plots of data indicated, the drug release profile of all dissolution in the pH-alternating system were not fitted to any of the models mentioned above. Therefore, it can be concluded that the release of the drug in each dissolution medium was controlled by a different mechanism.

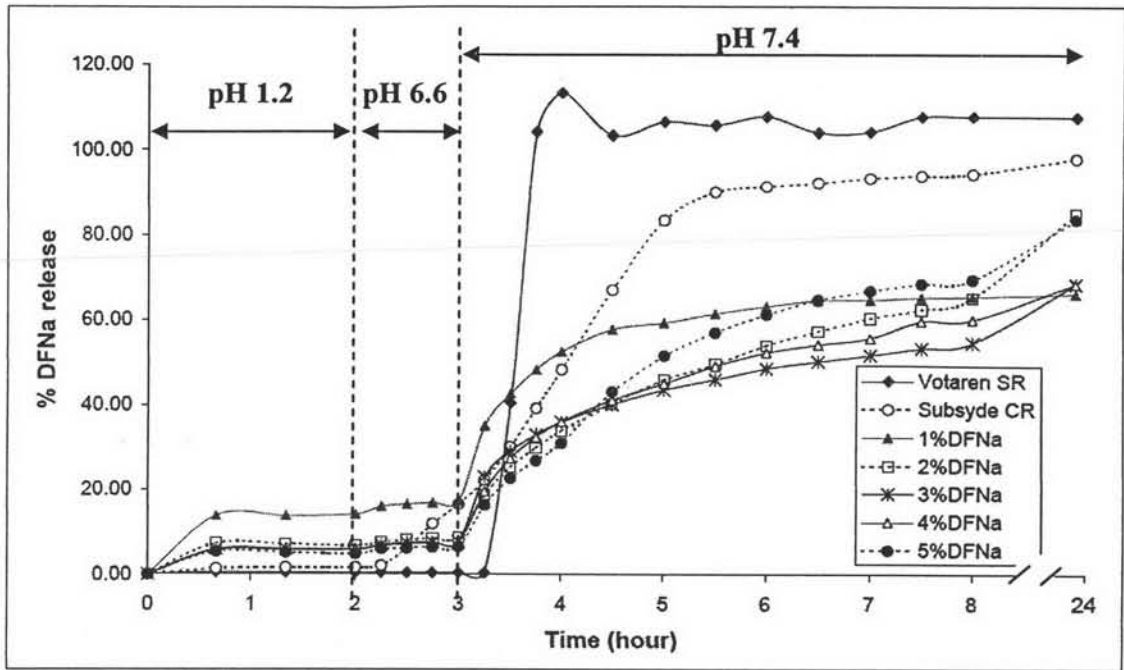


Figure 4.32 The dissolution profiles of sodium diclofenac from the chitosan/carrageenan (CS/CR : 2/1) beads with various drug content (%w/v) in the pH-alternating system.

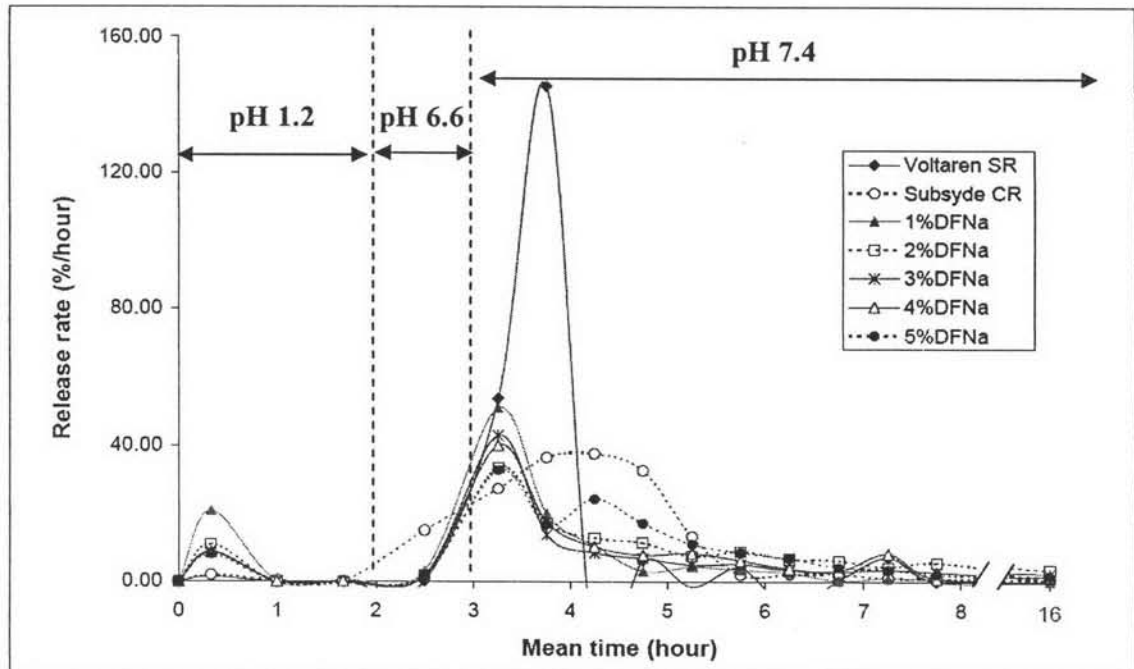


Figure 4.33 The release rate profiles of sodium diclofenac from the chitosan/carrageenan (CS/CR : 2/1) beads with various drug content (%w/v) in the pH-alternating system.

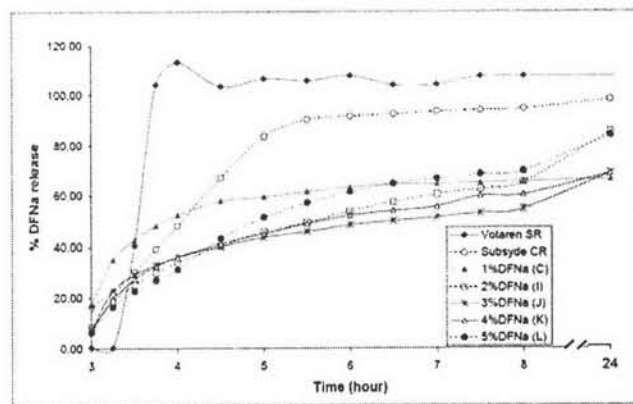
In the dissolution medium pH 1.2 (during the first-second hour), the drug release profile of the beads was not fitted to any of the aforementioned models (Figure 4.32, 4.33). About 7-16% of drug was released unpreferably. This can be presumed that the unencapsulated drug was immediately released from the bulk powder (Figure 4.27).

In the dissolution medium pH 6.6 (during the second-third hour), the percentage of the drug release of the beads and Voltaren[®] SR were not significantly increased. Whereas, Subsyde[®] CR started to release drug during pH 6.6.

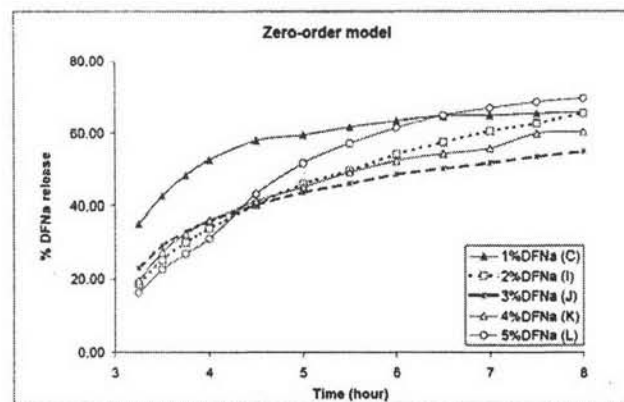
In the dissolution medium pH 7.4 (after the third hour), the drug release patterns were analyzed. None of the plots can be statistically fitted to any of the single-component kinetic model. Table 4.5 showed the values of correlation coefficient for all formulations, in which none was close to 1. For example, Figure 4.34 showed the plots of the different kinetic models from the dissolution profiles of the chitosan/carrageenan (CS/CR : 2/1) beads with various drug content (1-5 % (w/v)). The results showed that the plots were not linear. Therefore were not fitted to any model.

Table 4.5 Correlation coefficient of the relationships between percentage of drug released versus time (zero-order model), log percentage drug remained versus time (first-order model), and percentage drug released versus square root time (Higuchi model) of the single-component model

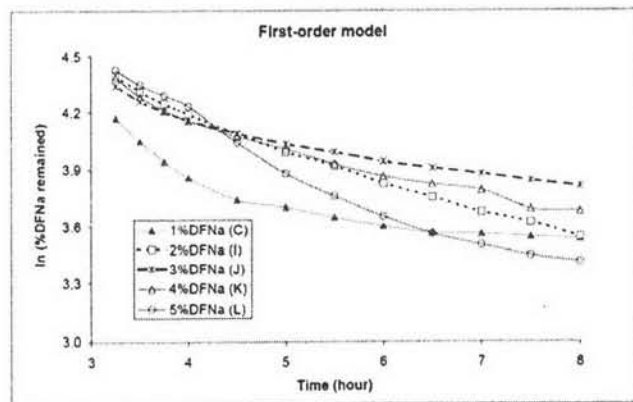
Formulation	Correlation coefficient		
	Zero-order	First-order	Higuchi
Voltaren SR	0.3108	0.3300	0.3478
Subsyde CR	0.8014	0.9217	0.8445
A	0.5964	0.6316	0.6443
B	0.5961	0.6312	0.6441
C	0.7711	0.8310	0.8147
D	0.6927	0.7405	0.7404
I	0.9518	0.9880	0.9730
J	0.9129	0.9492	0.9410
K	0.9200	0.9634	0.9464
L	0.9139	0.9633	0.9432
O	0.8012	0.8790	0.8746
P	0.8883	0.9195	0.9191
Q	0.9082	0.9417	0.9374
R	0.9100	0.9405	0.9386
S	0.9905	0.9994	0.9984



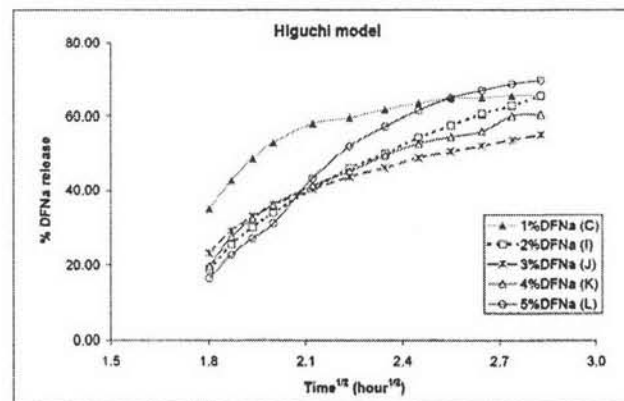
(a)



(b)



(c)



(d)

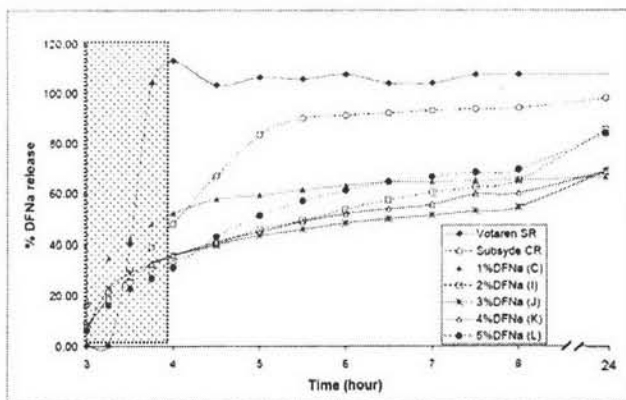
Figure 4.34 (a) The dissolution profiles, (b) zero-order model, (c) first-order model and (d) Higuchi model of sodium diclofenac from the chitosan/carrageenan (CS/CR : 2/1) bead with various drug content (1-5 %(w/v)) in the dissolution medium pH 7.4.

In contrast, the two-component model gave the value of the correlation coefficient closer to 1 than the single-component model (Table 4.6). For example, Figures 4.35 and 4.36 showed the plots of the different kinetic models from the dissolution profiles of the chitosan/carrageenan (CS/CR : 2/1) beads with various drug content (1-5 % (w/v)) during the third – fourth hour and after the fourth hour, respectively. The results showed that the plots of the two-component model was more linear than that of the single-component model.

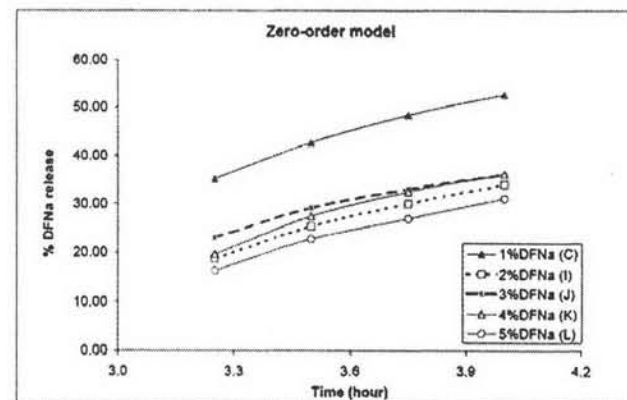
Table 4.6 Correlation coefficients of the relationships between percentage drug released versus time (zero-order model), log percentage drug remained versus time (first-order model), and percentage drug released versus square root time (Higuchi model) of the two-component model

Formulation	Correlation coefficient					
	During the third-fourth hour			After the fourth hour		
	Zero-order	First-order	Higuchi	Zero-order	First-order	Higuchi
Voltaren SR	0.9371	0.8424	0.9418	-	-	-
Subsyde CR	0.9988	0.9916	0.9976	0.6426	0.8265	0.6448
A	0.8321	0.8494	0.8428	0.7498	0.7532	0.7778
B	0.8319	0.8492	0.8426	0.7495	0.7529	0.7776
C	0.9839	0.9934	0.9875	0.9061	0.9172	0.9273
D	0.9646	0.9765	0.9699	0.6984	0.7123	0.7225
I	0.9850	0.9916	0.9884	0.9812	0.9959	0.9904
J	0.9737	0.9817	0.9784	0.9761	0.9869	0.9867
K	0.9711	0.9813	0.9761	0.9715	0.9825	0.9813
L	0.9870	0.9926	0.9900	0.9105	0.9527	0.9322
O	0.9447	0.9558	0.9516	0.9655	0.9733	0.9782
P	0.9708	0.9774	0.9757	0.9796	0.9858	0.9891
Q	0.9865	0.9908	0.9897	0.9674	0.9795	0.9786
R	0.9791	0.9853	0.9832	0.9725	0.9819	0.9840
S	0.9987	0.9976	0.9974	0.9959	0.9998	0.9994

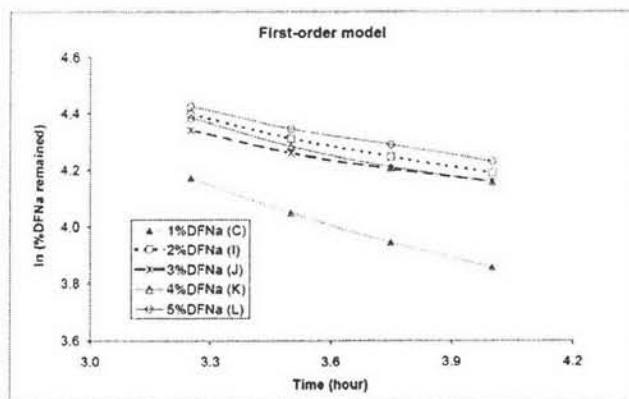
^a The drug was completely released within the first hour.



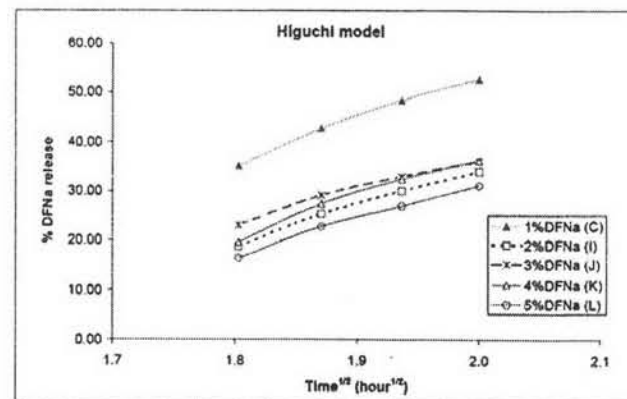
(a)



(b)

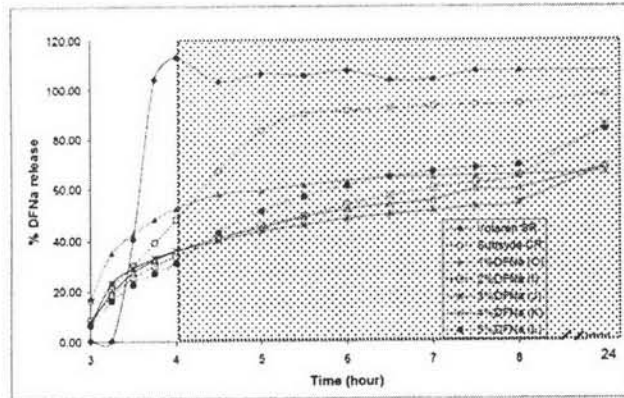


(c)

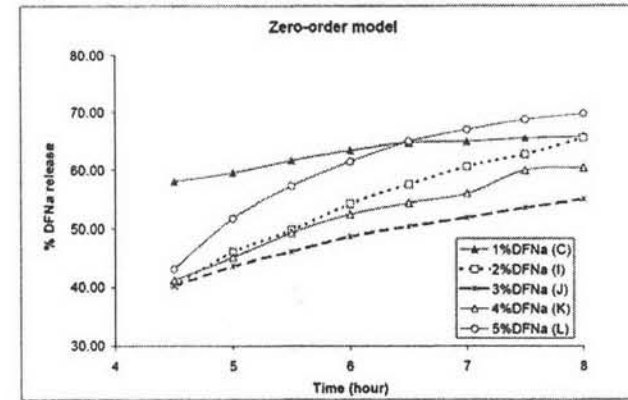


(d)

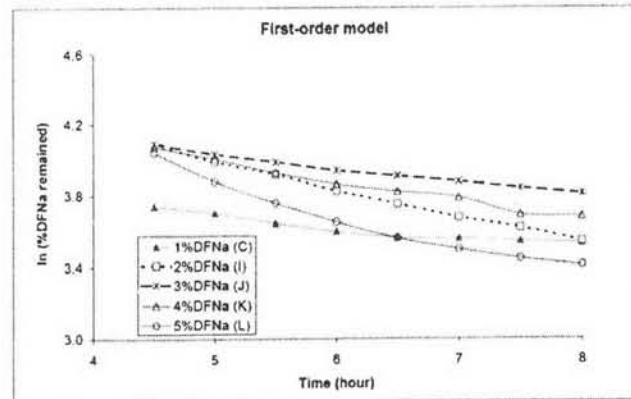
Figure 4.35 (a) The dissolution profiles, (b) zero-order model, (c) first-order model and (d) Higuchi model of sodium diclofenac from the chitosan/carrageenan (CS/CR : 2/1) bead with various drug content (1-5 % (w/v)) in phosphate buffer saline pH 7.4 during the third-fourth hour.



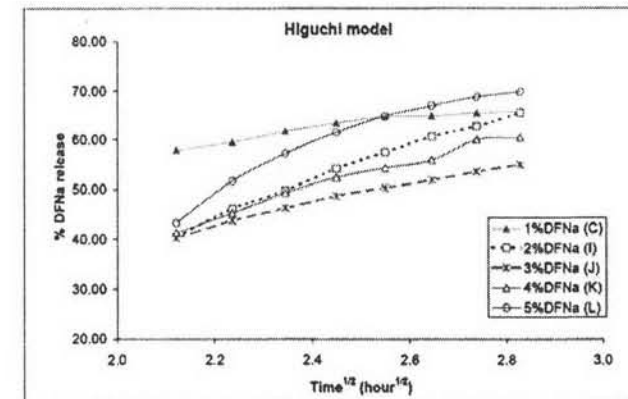
(a)



(b)



(c)



(d)

Figure 4.36 (a) The dissolution profiles, (b) zero-order model, (c) first-order model and (d) Higuchi model of sodium diclofenac from the chitosan/carrageenan (CS/CR : 2/1) bead with various drug content (1-5 %(w/v)) in phosphate buffer saline pH 7.4 after the fourth hour.

The determination of the drug release model was performed in phosphate buffer saline pH 7.4 by the two-component model, during the third – fourth hour and after the fourth hour.

When both the Higuchi plot and the first-order plot were nearly linear, it was necessary to differentiate between these two models. Therefore, the method of Benita and Donbrow^[22] was adopted for deciding the most appropriate model. In this method, if the plot of the drug release rate (dQ/dt) versus reciprocal percentage of drug release ($1/Q$) is more linear or produces a higher value of correlation coefficient than that obtained from the plot of rate of release versus percentage of drug release (Q), it means that the release profile was best fitted to the Higuchi model rather than the first-order model. Table 4.7 showed the correlation coefficient of the plots from this method.

Table 4.7 Comparison of linearity as plots of the release rate of the drug versus the reciprocal amount ($1/Q$) and the amount of sodium diclofenac release (Q) from the beads

Formulation	Correlation coefficient			
	During the third-fourth hour		After the fourth hour	
	Q	$1/Q$	Q	$1/Q$
A	0.9344	0.9115	0.8407	0.8470
B	0.9336	0.9105	0.7235	0.8468
C	0.8862	0.9464	0.7228	0.7331
D	0.9511	0.9268	0.4701	0.4682
I	0.9736	0.9968	0.8697	0.8854
J	0.9108	0.9682	0.9191	0.9434
K	0.9960	0.9861	0.4965	0.5104
L	0.9235	0.9756	0.9923	0.9860
O	0.9973	0.9928	0.8440	0.8578
P	0.9185	0.9664	0.8530	0.8791
Q	0.8477	0.9232	0.7058	0.7247
R	0.9036	0.9551	0.9307	0.9321
S	0.7356	0.9830	0.9122	0.9193

In the phosphate buffer saline pH 7.4, during the third-fourth hour, Formulation A, B, D and K gave the correlation coefficient of the drug release rate versus Q was higher than those of rate versus $1/Q$ as indicated in the first-order model. The other formulations gave the higher of the correlation coefficient from the drug release rate versus Q as followed Higuchi model.

The best fit of both the first-order and Higuchi plots from these formulations can be explained, the release of the drug in this period was controlled by the mechanism of the dissolution of DFNa in the dissolution medium together with the diffusion of drug through hydrogel bead.

However, in the phosphate buffer saline after the fourth hour, the correlation coefficient of the drug release rate versus Q and versus $1/Q$ showed no statistically significant difference (Table 4.7). From the example of the dissolution profiles of the beads given in Figure 4.36 (a), the release of drug was slowly increased because it was controlled by the mechanism of the diffusion of the drug through the hydrogel beads. Therefore, the model of this section might be the Higuchi model.